Electronics **2014**, *3*, 43-75; doi:10.3390/electronics3010043

OPEN ACCESS

electronics

ISSN 2079-9292

www.mdpi.com/journal/electronics

Review

Integration of Organic Light Emitting Diodes and Organic Photodetectors for Lab-on-a-Chip Bio-Detection Systems

Graeme Williams *, Christopher Backhouse and Hany Aziz

Department of Electrical and Computer Engineering & Waterloo Institute for Nanotechnology, University of Waterloo, 200 University Avenue, Waterloo, ON, Canada, N2L 3G1;
E-Mails: chris.backhouse@uwaterloo.ca (C.B.); h2aziz@uwaterloo.ca (H.A.)

***** Authors to whom correspondence should be addressed; E-Mail: g3willia@uwaterloo.ca; Tel.: +1-519-888-4567 (ext. 34803).

Received: 11 December 2013; in revised form: 15 January 2014 / Accepted: 27 January 2014 / Published: 13 February 2014

Abstract: The rapid development of microfluidics and lab-on-a-chip (LoC) technologies have allowed for the efficient separation and manipulation of various biomaterials, including many diagnostically relevant species. Organic electronics have similarly enjoyed a great deal of research, resulting in tiny, highly efficient, wavelength-selective organic light-emitting diodes (OLEDs) and organic photodetectors (OPDs). We consider the blend of these technologies for rapid detection and diagnosis of biological species. In the ideal system, optically active or fluorescently labelled biological species can be probed via light emission from OLEDs, and their subsequent light emission can be detected with OPDs. The relatively low cost and simple fabrication of the organic electronic devices suggests the possibility of disposable test arrays. Further, with full integration, the finalized system can be miniaturized and made simple to use. In this review, we consider the design constraints of OLEDs and OPDs required to achieve fully organic electronic optical bio-detection systems. Current approaches to integrated LoC optical sensing are first discussed. Fully realized OLED- and OPD-specific photoluminescence detection systems from literature are then examined, with a specific focus on their ultimate limits of detection. The review highlights the enormous potential in OLEDs and OPDs for integrated optical sensing, and notes the key avenues of research for cheap and powerful LoC bio-detection systems.

Keywords: lab-on-a-chip; organic electronics; organic light emitting diode; OLED; organic photodiode; OPD; point-of-care; photoluminescence

List of Abbreviations

Abbreviation	Full Name
abs	absorbance
Alq3	tris(quinolinolate) Al
a-NPD	*N*,*N*'-di(alpha-naphthyl)-*N*,*N*'-diphenyl-1,1'-biphenyl-4,4'-diamine
APD	avalanche photodiode
APnEOs	alkylphenol polyethoxylates
BCP	bathocuproine
BHJ	bulk heterojunction
Bphen	4,7-diphenyl-1,10-pheranthoroline
C545T	coumarin 545T
C60	fullerene
CBP	4,4'-Di(*N*-carbazolyl)biphenyl
CC-125	chlamydomonas reinhardtii
CCD	charge-coupled device
CL(q)	chemiluminescence (quenching)
CPPO	bis (2-carbopentyloxy-3,5,6-trichlorophenyl) oxalate
CuPc	copper phthalocyanine
DBR	distributed Bragg reflector
DCM	4-dicyanomethylene-2-methyl-6-(*p*-dimethylaminostyril)-4H-pyrane
DCMU	3(3,4-dichlorophenyl)-1,1-dimethylurea, Diuron
DMAP	4-dimethylaminopyridine
DPVBi	4,4'-bis(2,2'-diphenylvinyl)-1,1'-biphenyl
EL	electroluminescence
EP	electrophoretic
EQE	external quantum efficiency
HPTS	8-hydroxypyrene-1,3,6-trisulfonic acid
IEF	isoelectric focusing
Ir(ppy)3	tris(2-phenylpyridine)iridium
IV	current-voltage (measurements)
LIF	laser-induced fluorescence
LoC	lab-on-a-chip
LoD	limit of detection
MEH-PPV	poly[2-methoxy-5-(2'-ethylhexyloxy)-*p*-phenylene vinylene]
mIgG	mouse immunoglobulin G
mKP	m-Cresol purple
NHDF	normal human dermal fibroblasts
NPB/NPD	4,4'-bis[*N*-(1-naphthyl)-*N*-phenylamino]biphenyl
OLED	organic light emitting diode
OPD	organic photodetector
OSC	organic solar cell

List of Abbreviations (*Cont.*)

Abbreviation	Full Name
PBD	2-(4-biphenyl)-5-(4-*t*-butylphenyl)-1,3,4-oxadiazole
PC70BM	1-(3-methoxycarbonyl)-propyl-1-phenyl-(6,6)C71
PCBM	1-(3-methoxycarbonyl)-propyl-1-phenyl-(6,6)C_{61}
PCDTBT	poly [N-9'-heptadecanyl-2,7-carbazole-alt-5,5-(4',7'-di-2-thienyl-2',1',3'-benzothiadiazole)]
PDMS	polydimethylsiloxane
PDY-132	Super Yellow
PEDOT:PSS	poly(3,4-ethylenedioxythiophene) poly(styrenesulfonate)
PF	polyfluorene
PL(q)	photoluminescence (quenching)
PMT	photomultiplier tube
PMMA	poly(methyl methacrylate)
PP	polypropylene
PPV	poly(*p*-phenylene vinylene)
PTCBI	3,4,9,10-perylenetetracarboxylic bis-benzimidazole
PtOEP	Pt octaethylporphyrin
PtTFPP	(II) meso-tetra(pentafluorophenyl)porphine
PVK	poly(9-vinylcarbazole)
Rh6G	rhodamine 6G
RhB	rhodamine B
rhTSH	recombinant human thyroid stimulating hormone
RIU	refractive index unit
Ru(dpp)	tris(4,7-diphenyl-1,10-phenanthroline) Ru chloride
SEB	staphylococcal enterotoxin B
SNR	signal to noise ratio
SPR	surface plasmon resonance
TAC	total antioxidant capacity
TAMRA	tetramethylrhodamine
TOA+OH-	tetraoctylammonium hydroxide
μTPD	*N*,*N*'-diphenyl-*N*,*N*'-di(m-tolyl)-benzidine
μc-OLED	microcavity OLED

1. Introduction

Substantial research efforts have been dedicated to the development of lab-on-a-chip (LoC) technologies, which have matured in parallel with the many advances in the field of microfluidics. LoC offers a miniaturized platform for sample processing and can be used to perform numerous life sciences analyses. The labour intensive steps associated with common detection and biomaterial processing schemes (for example, detection and isolation of specific DNA strands, antibodies or pathogens) can be feasibly simplified to a one-step sample injection into a microfluidic well. The appeal of LoC is thus a combination of the following: a reduction in user error, a decrease in materials/sample usage, fast and low cost analysis, and potential automation of routine techniques.

While there have been numerous breakthroughs in the microfluidics of LoC bio-detection systems [1–3], much of the detection methodologies still rely on external lab-scale systems. However,

there is a strong desire for completely portable LoC systems for point-of-care applications. Given its high degree of sensitivity, many groups have sought to integrate fluorescence/photoluminescence (PL) detection techniques into LoC. In the current review, we examine LoC PL-based detection schemes that use organic light emitting diodes (OLEDs) as an excitation source and/or organic photodiodes (OPDs) as a means of detection.

Since OLEDs and OPDs are comprised of thin films deposited by low temperature techniques, they can be easily integrated with most polymer/plastic microfluidic systems (for example, by depositing on the backside of a polydimethylsiloxane (PDMS) microfluidic channel). The capability to fabricate miniaturized OLED pixels is also ideal for LoC, where the microchannel size can be on the order of an individual pixel size [4,5]. Further, the emission and absorption peaks of OLEDs and OPDs respectively are easily tunable—dependent on the choice of small molecule or polymer—so these organic electronic devices are excellent candidates for more advanced detection systems, such as multiplexed immunoassays using multiple PL peaks. This review is organized as follows: the common OLED and OPD device structures, as well as their principles of operation, are discussed in Section 2. Notable developments in optical excitation and detection methods for non-OLED/OPD LoC technologies are detailed in Section 3, highlighting the potential advantages of OLED and OPD integration. Integrated systems employing OLEDs and/or OPDs in LoC technologies will then be addressed in Section 4.

2. Operation Principles of Organic Light Emitting Diodes and Organic Photodetectors

Organic electronic devices employ highly conjugated organic species that are divided into two material subsets: small molecules and polymers. In terms of their implementation, small molecule species are historically insoluble and are thus commonly vacuum-deposited by thermal evaporation techniques. In contrast, polymer materials are more easily synthesized to be soluble in common organic solvents. As an addendum to this point, while they are difficult to synthesize, soluble small molecules are feasible and have recently become the subject of intense research [6–8]. Some of the earliest and most studied OLED materials include tris(quinolinolate) Al (Alq_3) and 4,4'-bis[*N*-(1-naphthyl)-*N*-phenylamino]biphenyl (NPB/NPD) for small molecule devices [9,10], and poly(*p*-phenylene vinylene) (PPV) derivatives for polymer devices [11]. As a point of note, Alq_3 films electroluminesce with a peak wavelength of 530 nm, whereas poly[2-methoxy-5-(2'-ethylhexyloxy)-*p*-phenylene vinylene] (MEH-PPV), a common PPV derivative, emits at 600 nm with a shoulder emission at 640 nm. As an excitation source for LoC applications, the OLED's peak emission must be chosen appropriately to excite the known fluorophore without substantially overlapping the detector's absorption spectrum. From a fabrication standpoint, this is simple to envision, as there now exist OLED materials with peak emission over the entire visible spectrum—in fact, Alq_3 on its own can be tailored to emit over most of the visible spectrum [12]. To this end, the position of each organic material's absorption and emission peak is fundamentally related to its chemical structure (especially its degree of conjugation), which can be altered during its synthesis.

Early and common OPD materials include copper phthalocyanine (CuPc), 3,4,9,10-perylenetetracarboxylic bis-benzimidazole (PTCBI) and fullerene (C_{60}) for small molecule OPDs [11], and MEH-PPV and 1-(3-methoxycarbonyl)-propyl-1-phenyl-(6,6)C_{61} (PCBM) for polymer OPDs [13].

In OPDs, the hole transport layer and electron transport layer are commonly referred to as the donor and acceptor respectively, in light of their typical roles in the device (where the donor 'donates' a free electron to the acceptor). The donor and acceptor are commonly mixed together to form a bulk heterojunction (BHJ). In principle, simple OPDs have the same structure as organic solar cells (OSCs)—the difference lies in their mode of operation, where OPDs can be negatively biased to enhance free carrier transport. It is therefore logical that many polymer-based OPDs now make use of the ubiquitous poly3-hexylthiophene (P3HT):PCBM BHJ, which is famous for its use in OSCs [14]. Since OPDs are largely adapted from OSC technologies, they absorb strongly over most of the visible spectrum—for example, P3HT:PCBM OPDs generate substantial photocurrent between 350 nm and 650 nm. For LoC applications, the peak absorption of the OPD should correspond well with the fluorophore's emission spectrum, but it should ideally not overlap with the emission from the excitation source.

Illustrations of the general device structures and energy level diagrams of an OLED, a simple bilayer OPD and a mixed layer/BHJ OPD are provided in Figure 1A–C respectively. Each device comprises an electron transport layer (ETL, or an acceptor in the OPD) and a hole transport layer (HTL, or a donor in the OPD), and the OLED may have an additional emissive layer (EML). Note that the energy levels of the metal and ITO layers are their work functions, whereas the energy levels of the organic layers are their highest occupied molecular orbitals (HOMOs) and lowest occupied molecular orbitals (LUMOs). In an even simpler incarnation of the OLED device—the bilayer OLED—either the hole transport layer or the electron transport layer may serve a dual role as the emissive layer. A simple example of this is the ITO/NPB/Alq_3/MgAg bilayer OLED. Devices may also make use of additional hole injection/extraction layers (HILs, HELs) and electron injection/extraction layers (EILs, EELs). These are not illustrated in the energy level diagrams, but they are typically few-nm layers (e.g., 5 nm MoO_3, 1 nm LiF) used to adjust the electrode work functions and/or to provide enhanced device stability [15–17].

Figure 1. Illustration of the common device structures and associated energy level diagrams for a(n) (**A**) organic light emitting diode (**B**) bilayer organic photodetector (**C**) bulk heterojunction organic photodetector.

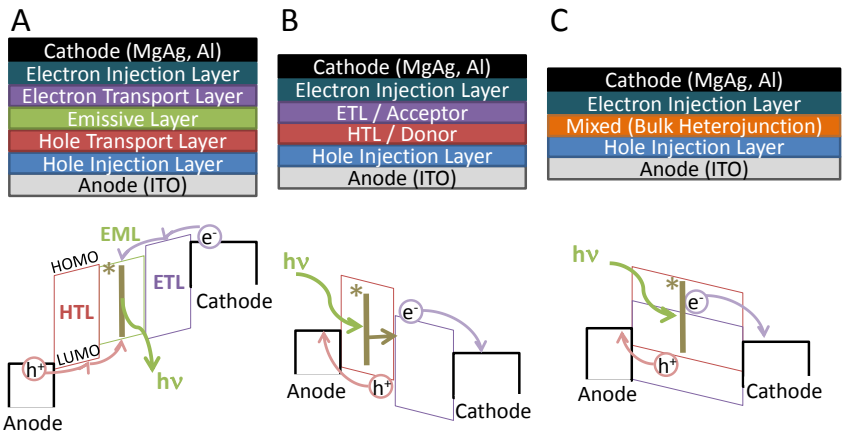

As illustrated in Figure 1A, OLED devices operate as follows:

- A negative bias is applied to the cathode / a positive bias is applied to the anode
- A hole is injected (either by thermionic or field emission) into the HTL and an electron is similarly injected into the ETL
- The electron and hole meet in the EML, form an exciton (denoted as *|), and recombine to emit a photon with energy hν, proportional to the energy gap of the emissive layer.

OPDs operate in approximately the reverse manner, as illustrated in Figure 1B,C, where a photon generates an exciton that is dissociated at a donor-acceptor interface. The specific operation of the OPD is as follows:

- A negative bias is applied to the anode / a positive bias is applied to the cathode
- A photon is absorbed by either the donor or acceptor material (in Figure 1, the photon is absorbed by the donor material) to generate an exciton (denoted as *|)
    - the exciton traverses to the donor/acceptor interface to dissociate into its constituent electron and hole
- The electrons and holes travel along the ETL and HTL to be collected at the cathode and anode respectively.

One of the main limitations to OPD efficiency in the simple bilayer device is the diffusion of the exciton from its point of excitation to the donor/acceptor interface (*i.e.*, before the exciton undergoes recombination). The BHJ architecture serves to minimize exciton diffusion length with an interpenetrating network of donor and acceptor, granting a large number of donor/acceptor interfaces throughout the entire device structure. Unfortunately, this architecture also serves to substantially increase the OPD leakage current since holes can be injected directly from the cathode to the donor HOMO and electrons can be injected directly from the anode to the acceptor LUMO. This effect, however, is avoidable by using a BHJ bordered by neat donor and acceptor layers, referred to as the planar-mixed molecular heterojunction (PM-HJ) [18]. Alternatively, this effect can be minimized through use of carrier-selective extraction layers [19].

The majority of organic electronics research to date has focused on optimization of device performance. For OLEDs, this implies high brightness values through high external quantum efficiencies, with a focus on phosphorescent OLEDs that can show substantial efficiency improvements compared to their fluorescent counter-parts due to electron/hole spin statistics [20]. For OPDs, this implies high ‘on-off’ ratios and, similarly, high external quantum efficiencies, which has been largely addressed with the design of intelligent device architectures [11]. For LoC applications, other critical and less researched device optimizations must also be addressed, such as reducing the full width at half maximum (FWHM) of the OLED emission, and identifying new materials systems for OPDs with narrow regions of absorption. Both efforts should serve to reduce the system dark noise by decreasing light leakage from the excitation source to the detector, ultimately allowing for better detection limits. A final consideration for the use of OLED or OPD detection systems in commercial LoC applications relates to the stabilities of the organic optical elements. However, with proven manufacturability of both OLEDs and OSCs from companies such as Samsung and Heliatek, as well as

a demonstrated potential for extremely long device lifetimes [21,22], it is clear that both OLEDs and OPDs have promise for use in point-of-care LoC systems.

3. Early Integration of Optical Excitation and Detection into Lab-on-a-Chip

The vast majority of LoC research to date has been dedicated to finer manipulation of relevant biological species through smart microfluidics. Comprehensive reviews on this particular topic have been presented elsewhere [1–3,23–26]. The culmination of this work is a portfolio of tried and proven microfluidic channels, with a strong understanding of their fabrication methodologies. These channels are generally integrated with larger lab-scale excitation/detection systems. With a greater competency in the control of various biological species, many researchers have now shifted their focus toward integration of these channels with optical manipulation and detection techniques [27–30]. Consider a lab-scale laser-induced fluorescence (LIF) detection setup as it may be incorporated with a microfluidic system, illustrated in Figure 2, and for which numerous research articles have been published [31–34]. In the setup illustrated in Figure 2, the biological species of interest first flow through a microfluidic channel to the relevant point of detection. These species are excited by a blue laser that is focused onto the channel using mirrors and objective lenses. As the excited species relax they emit green light, which is captured by a collection lens, collimated, filtered and routed to a photomultiplier tube (PMT). Some enhancements to this system have been proposed, such as the inclusion of microlenses or wavelength-selective optical waveguides for fine control of the excitation or emitted light [35,36]. While these enhancements allow one to probe multiple channels simultaneously, they also greatly complicate device fabrication.

Figure 2. Example laser-induced fluorescence setup when integrated with a microfluidic system for detection of biological species labelled with a fluorescent dye. Figure re-used from Ref. [32] with permission, copyright 2006 American Chemical Society.

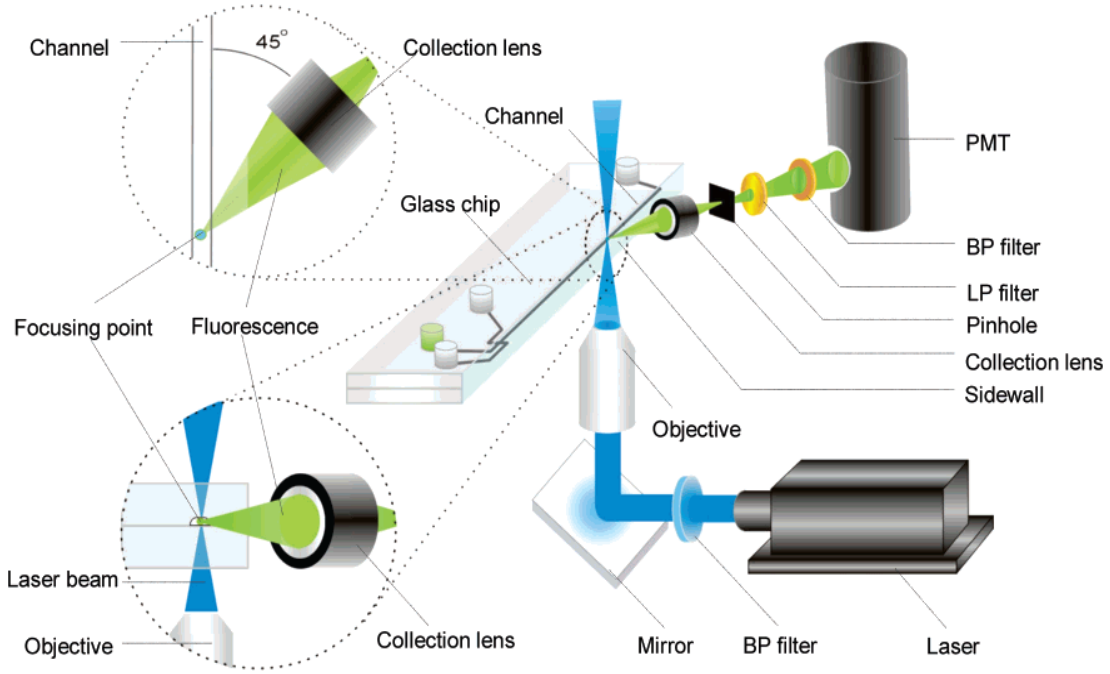

The inherent difficulty with these systems is immediately apparent: each system requires complicated and costly optics for excitation and subsequent photoluminescence detection. Beyond the large size of such a set-up, these systems are extremely sensitive to variations in the positioning of the optical components. Fu *et al.* studied the optimal laser-detector orientation, finding that a 45 ° light collection angle to the direction of flow (and 90 ° to the excitation source, as illustrated in Figure 2) offered the best signal to noise ratio (SNR) [32]. While these systems provide impressive results, it is much more desirable to implement the miniaturized LoC technologies with, similarly, miniaturized test platforms. It is worth noting that the adjacent field of optofluidics, which marries optical probing techniques and associated optical phenomena with microfluidics, provides some hints as to how these test platforms may be constructed [37,38]. For example, Gersborg-Hansen and Kristensen developed distributed feedback (DFB) lasers based on third-order Bragg gratings, which also acted as microfluidic channels for their chosen laser dyes [39]. Such a system thus incorporates many of the core aspects of an OLED-/OPD-based LoC system, such as photon generation from organic species and subsequent photon waveguiding.

As a means to better appreciate the advantages of OLED- and OPD-based excitation/detection systems, it is useful to examine current integration schemes that do not employ OLEDs or OPDs. One of the most notable approaches makes use of optical fibres to either route the excitation light to the analyte, or to extract the emitted light from the fluorophore. For example, Chabinyc *et al.* developed a miniaturized test platform where excitation light is fed through optical fibre to PDMS microchannels [40]. Their approach is further unique as it makes use of a micro-avalanche photodiode (μAPD), which is encapsulated in PDMS and placed directly underneath microfluidic channels. Since the μAPD is in such close proximity to the fluorophore, lenses and concentrators are not required. Using this approach, Chabinyc *et al.* were able to detect a minimum concentration of 25 nM fluorescein, and they were able to separate and detect proteins by capillary zone electrophoresis. The main limitation to this approach is the complexity in device fabrication, especially in consideration of the fragile μAPDs and of the difficulty in optical fibre alignment. OLEDs and OPDs may offer a solution to this problem as they can be deposited adjacent to the microchannel and thus do not require any direct physical alignment or manipulation.

Irawan and coworkers also pursued a fibre-coupling scheme to microfluidic devices with some success [33,41,42]. In their preliminary work, the authors made use of a poly(methyl methacrylate) (PMMA) optical fibre and lamination methods to couple blue LED excitation light to their microchannels [41]. Combined with a charge-coupled device (CCD) detector (including relevant filters, lenses and pinhole masks), the researchers managed to detect fluorescein at concentrations of ~3 nM. Irawan *et al.* later improved upon this work, implementing groove-cut PMMA optical fibres to allow for emission from several points along the fibre [33]. As shown in Figure 3, this allows for integration of the fibre into a multi-channel microfluidic device. This research resulted in detection of 30 pM of fluorescein.

Figure 3. (**A**) Illustration of the groove-cut optic fibre excitation methodology for PL detection in lab-on-a-chip applications. (**B**) SEM micrograph of the groove-cut optic fibre. Figures re-used from Ref.'s [33] and [42] with permission, copyright 2007/2009 Springer.

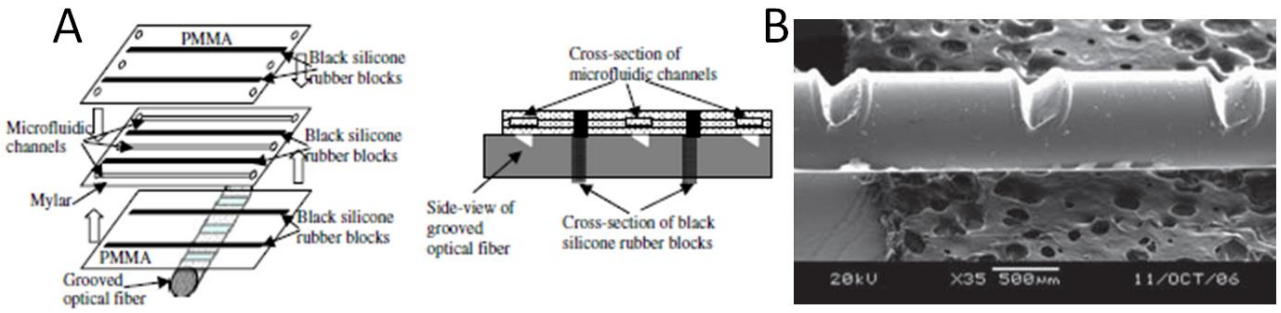

Numerous other approaches to couple light into and out of microfluidic channels have been tested. For example, in order to bypass the difficulty of integrating optical fibres into LoC microfluidics, Seo and Lee instead used 2D-patterned microlenses to couple blue LED excitation light into their microchannels [43]. This follows the work of Roulet and coworkers noted earlier [35], but with a much simpler implementation and without the need for a laser excitation source. Mazurczyk *et al.* fabricated channel optical waveguides with the use of an ion exchange technique in soda lime glass substrates to achieve efficient coupling of light into their microchannels [44]. Instead of coupling light to the microfluidic channels directly, Novak and coworkers aimed to miniaturize the testing platform, effectively achieving a fluorescein detection limit of ~2 nM [45]; however, this approach still requires costly filters and lenses. Ryu *et al.* followed a similar approach, but removed the lenses and used (relatively cheap) dye coated colour filters and linear/reflective polarizers to improve SNR [46], ultimately granting a fluorescein detection limit of ~3 nM. The use of polarizers in LoC systems is a relatively cheap and effective method to remove excitation light before it reaches the detector. This method relies on the placement of orthogonally oriented linear polarizers at both the excitation source and the detector. To this end, linearly polarized light from the excitation source interacts with the fluorescent analyte, resulting in the emission of non-polarized light. While the non-polarized light can pass the second polarizer to reach the detector, the excitation light is blocked due to its orthogonal polarization.

The common theme in all attempts to integrate PL sensing with LoC is the difficulty associated with in-coupling the excitation light and out-coupling the emitted light. In order to achieve a high SNR and a high limit of detection, the intensity of light impingent on the fluorophores must be high. This allows for measurable signals even from highly dilute species. Furthermore, a significant portion of light emitted from the fluorophore must subsequently reach the detector. While the LoC systems studied in this section offer creative and effective methods for light incoupling and outcoupling, these methods largely rely on complicated and, ultimately, costly extra microchannel fabrication steps. For manufacturability, system compatibility and overall simplicity in LoC bio-detection systems, it behooves us to examine easily implementable and more modular designs. In this manner the microfluidics can be fabricated first and then subsequently married to the optimized optical excitation and detection schemes. OLEDs and OPDs may prove to satisfy this requirement, as they can be

deposited directly on already-fabricated microchannels, or they may easily be fabricated on separate substrates that can be bonded to PDMS microchannels.

4. Integrated Organic Light Emitting Diode and Organic Photodetector Lab-on-a-Chip Systems

The appeal of OLEDs and OPDs for LoC stems from their potential ease of integration. As briefly discussed in Section 2, the most costly aspects of a PL detection system are generally associated with the optics required to have strong excitation output powers and high collection efficiencies. By placing the excitation source and the detector adjacent to the microchannels of interest, one may potentially eliminate the need for lenses, for detectors with internal gain (APDs or PMTs) and for strict alignment. This shifts this technology's realm of applicability from the lab-scale environment to a miniaturized, modular, point-of-care sensing platform.

OLEDs and OPDs, however, are not unique in their ease of linking to adjacent pre-fabricated microchannels. For example, there has been some success making use of hydrogenated amorphous silicon (a-Si:H) photodetectors toward the same goal [47,48]. In this regard, both a-Si:H and organics can be deposited in low temperature environments and can be deposited on top of common microfluidic materials (for example, PDMS). As such, OLEDs, OPDs and a-Si:H PDs can all can be optimized separately and joined to the microfluidics in a modular fashion. Further, all technologies can be miniaturized into individual pixels for sensor array applications. However, OPDs have an added benefit over a-Si:H PDs, as their absorption spectra can be tuned by the use of different organic materials. Combined with the tunable OLED emission spectra, OLED-OPD-LoC systems could feasibly be used to sense multiple PL peaks from different biological species within the same microchannel.

A critical limitation toward integrated PL sensing in any LoC system is the requirement for low noise and thus high SNR. For an OLED-OPD-LoC system, given the proximity of the OLED to the OPD, detection of the OLED excitation light by the OPD can be a significant contribution to noise. There exist several nascent techniques that may be used to minimize or even eliminate this problem. One may:

- use micro-cavity effects (with a semi-reflective anode instead of the transparent anode shown in Figure 1) or distributed Bragg reflectors (DBRs) to substantially narrow the FWHM of the OLED emission peak and remove tail-end emission
    - See, for example, [49,50] for micro-cavities based on metal mirror electrodes and [51] for micro-cavities based on dielectric quarter-wave stack (QWS) mirrors.
- operate the OLED in pulsed mode and exploit differences in electroluminescence (EL) response/decay time *versus* the fluorophore PL response/decay time
    - If the OLED and the fluorophore are selected appropriately, it may be feasible to offset the OLED's emission and the OPD's detection.
    - In some cases, high current pulse operation has allowed for very high brightness values in OLEDs, which may further enhance PL [52].
- use clever design techniques to minimize the excitation light coupled into the OPD
    - For example, see Figure 4, which is a suggested back-detection device and is discussed further below. Shinar and coworkers used a much simpler implementation of a

back-detection device (with a PMT detector and with no efforts to block or shield excitation light) to some success for their oxygen sensors [53–57].

- incorporate thin film absorbers or polarizers (e.g., following work by Ryu *et al.* [46])
    - While these techniques are the simplest, they also serve to substantially decrease the intensity of the PL signal. They may therefore not be suitable to adequately reduce noise and to provide competitive SNR values that can compete with present lab-scale LIF systems.
    - To minimize the number of components required in the LoC system, it may be feasible to employ excitation sources that emit polarized light without the use of linear polarizers. Such excitation sources have recently been demonstrated with polymer emitting nanofibres, showing the potential for electrical excitation (when incorporated in polymer OLED-like devices) [58], as well as demonstrating reasonable integration into microfluidic systems [59].

Figure 4. Illustration of the structural layout of a potential back-detection OLED-OPD lab-on-a-chip system.

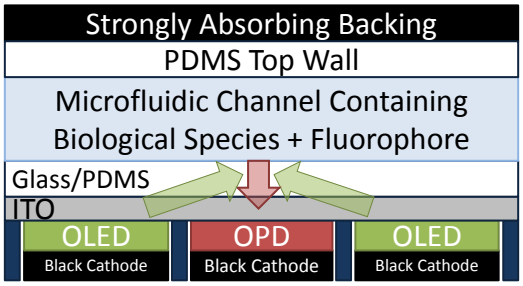

For the back-detection geometry shown in Figure 4, the OLED and OPD are fabricated on the same substrate, which can greatly simplify the fabrication process, and they are separated by opaque spacers. The OLEDs emit green light that interacts with the fluorophore to emit red light as detected by the OPD. By making use of a strongly absorbing backing and black cathodes (see, for example, [60,61]) one may minimize the amount of stray OLED light that reaches the OPD—essentially limiting it to partial reflections and waveguided light.

4.1. Organic Light Emitting Diode-Integrated Lab-on-a-Chip Systems

A summary of the LoC systems employing an OLED excitation source are provided in Table 1 (note: instead of an OLED, ref. [62] uses an organic semiconductor laser). The results have been grouped together by their specific application, which coincides with specific research groups/principal investigators. The intended applications of the various LoC systems in Table 1, and thus the analytes of interest, vary among the different research groups. As such, cross-comparisons on the efficacy of each system are difficult, and so both the analyte and the sensor's dynamic range are listed. For the cases where a dynamic range is not explicitly listed, values have been ascertained from figures within the publications. For entries with multiple publications, the best dynamic range from the group of publications is listed.

Table 1. Summary of lab-on-a-chip systems with OLED excitation sources.

Application		Micro-Fluidic	OLED Details	Detector	Analyte	Dynamic Range	Ref.
Dye conc	PL	PDMS channel	ITO/α-NPD/Alq_3/LiF/Al	CCD w/ fibre	RhB	5–100 μM	[63,64]
			ITO/α-NPD/ Alq_3:C6/Alq_3/LiF/Al				
Multi-analyte conc	PLq	film (non-MF), PP channel	ITO/CuPc/a-NPD/ DPVBi/Alq_3/CsF/Al	PMT, Si PD + pre-amp	glucose, lactate, ethanol	0.02–0.3 mM	[53–57,65]
			ITO/CuPc/a-NPD/ Alq_3/CsF/Al		O_2	0–100%	
			ITO/CuPc/NPD/Alq_3:C545T/Alq_3/LiF/Al		dissolved O_2	2–40 ppm	
EP sep'n, immune assay	PL	etched glass, PDMS channel	ITO/PEDOT:PSS/ (PF or PPV emitter) /LiF/Al	PMT, Si APD w/ filter, lens, fibre	fluorescein	1 μM–10 mM	[66,67]
					HSA	10–100 mg/L	
Dye conc, IEF	PL	PDMS channel	ITO/NPB/Alq_3/ Mg:Ag/Ag	PMT, CCD w/ filter, lens	rhodamine 6G, Alexa Fluor 532	50–700 μM	[68–70]
			commercial AM-OLED array		R-phyco-erythrin	38 ng/mL –50 μg/mL	
Dye conc, immune assay	PL	etched glass, PDMS channel	ITO/CuPc/α-NPD/Alq_3/LiF/Al	p-i-n, p+n PD	TAMRA	10–100 μM	[71,72]
					Rh6G	1–100 μM	
Analyte conc	IV	droplet	ITO/TPD/Alq_3/Al	N/A	ethanol, methanol	10–1E3 ppm	[73]
Dye conc	PL	PDMS channel	AZO/PEDOT:PSS/ PDY-132/Alq_3/Ag	spectro-meter	sulforho-damine 101	N/A	[74]
Dye conc, immuno assay	PL	PDMS channel	ITO/TPD/ CBP:Ir(ppy)$_3$/Bphen/ Alq_3/Mg:Ag/Ag	linear CCD w/ filter	resorufin	7.8 μM–80 μM	[75]
					IgA	17–100 ng/mL	
Dye conc	PL	PMMA channel	Alq_3:DCM on DFB gratings, pumped w/ UV laser	spectro-meter w/ filter, lens	fluoro-spheres, Alexa 647	N/A	[62]
Dye conc, immuno assay	PL	droplet	ITO/PEDOT:PSS/ α-NPB/PBD/LiF/Al	CCD w/ filter	Alexa 430	156–1E4 pg	[76]
					hTG2 antigen	200–5E3 pg	

Hofmann and coworkers studied a spincoated PPV-based polymer OLED (500 to 700 nm emission) as an excitation source [67]. The light from the OLED was focused onto a patterned PDMS microchannel using a biconvex lens, allowing for PL detection of labelled urinary human serum albumin (HSA) by a CCD spectrometer. Their efforts allowed for HSA detection from 10 to 100 mg/L.

Scholer *et al.* also investigated the use of a polymer OLED as an excitation source for LoC, but they instead used Super Yellow (PDY-132) as their polymer emitter. Combined with a spectrometer detector, they were able to successfully test for the presence of sulforhodamine 101 [74]. Instead of using polymer OLEDs, Camou *et al.* examined a ~530-nm emitting small molecule OLED excitation source deposited on a glass substrate and bonded back-to-back to a PDMS microchannel for detection of Rhodamine B [63,64]. This simpler approach removed the need for a focusing lens. Their OLED had the structure ITO/*N*,*N*'-di(alpha-naphthyl)-*N*,*N*'-diphenyl-1,1'-biphenyl-4,4'-diamine (α-NPD) (HTL)/Alq_3 (ETL & EML)/LiF (EIL)/Al. The researchers also used an optical fibre to route their fluorescent dye's emitted light to a CCD detector. The fibre was slid into a channel formed in the PDMS directly adjacent to the microchannel. Camou and coworkers were able to detect 10 μM solutions of Rhodamine B visually, and 50 μM solutions by the CCD detector.

Marcello and coworkers employed a similar OLED structure, but replaced the Alq_3 ETL with 2-(4-biphenyl)-5-(4-*t*-butylphenyl)-1,3,4-oxadiazole (PBD), which allows for blue light emission from α-NPD. They further chose a fluorophore, Alexa Fluor 430, which has a large Stokes shift (>100 nm), allowing for simpler removal of the excitation signal from their CCD detector. In spite of this deliberate design choice, their test array still required the use of a bandpass filter, thus highlighting the need for further system alterations, such as back-detection device geometries, that reduce the amount of excitation light that reaches the detector. Their system was shown to be capable of detecting 156 pg of Alexa 430 per droplet of solution, and the researchers extended their LoC system to an indirect antibody assay to detect 200 pg of hTG2 with good specificity.

Choudhury, Shinar and Shinar also investigated patterned blue OLED pixels as their excitation source [55]. EL was from 4,4'-bis(2,2'-diphenylvinyl)-1,1'-biphenyl (DPVBi) incorporated into the device: ITO/CuPc (HIL)/α-NPD (HTL)/DPVBi (EML)/Alq_3 (ETL)/CsF (EIL)/Al. They also examined green-emitting devices by replacing the DPVBi EML with Alq_3, effectively extending the Alq_3 ETL already present. 2 mm by 2 mm emitting pixels were formed in a passive matrix by the cross-hatch of patterned ITO and Al strips. Similar to the approach by Camou *et al.* [63,64], the OLED was fabricated on a glass substrate and bonded to the patterned PDMS microchannels. Choudhury and coworkers used their OLED-microchannel setup for the detection of glucose by dissolving glucose oxidase (GOx) in solution with an oxygen-sensitive dye. For blue-emitting OLEDs, tris(4,7-diphenyl-1,10-phenanthroline) Ru chloride (Ru(dpp)) was used, while Pt octaethylporphyrin (PtOEP) was used with the green-emitting OLEDs. At a certain oxygen concentration, PL of the dyes is largely quenched. However, the presence of glucose in the microfluidic channel results in its enzymatic oxidation by GOx and a local reduction in oxygen content. The decrease in oxygen content reduces the quenching of the dye, enabling it to emit, and thus allowing for the highly sensitive detection of glucose.

Cai and Vengasandra *et al.* of the same research group expanded upon this work to test for alcohol and lactate in addition to glucose with alcohol oxidase (AOx) and lactate oxidase (LOx) [56,57,65]. Some key data from this work is shown in Figure 5. The yellow-orange emission is due to the combined emission from the Alq_3 OLED as well at the PtOEP dye. As a point of interest, the EL decay time of the presently examined OLEDs is ~30 – 100 ns, while the decay time of Ru(dpp) PL is ~0.3 to 8 μs and that of PtOEP is on the order of ~100 μs. As noted previously, this difference in EL *vs.* PL decay time can be used to vastly improve SNR by offsetting the excitation and the detection. This system is thus ideal for PL lifetime measurements, which are illustrated in the sub-panels of Figure 5.

The decay time of the photoluminescence for each species relates to its concentration by use of a modified Stern-Volmer equation. For the experiment shown in Figure 5, liquid or sol-gel samples containing the relevant biological species were deposited into wells containing a pre-deposited polystyrene(PS):PtOEP or PS:TiO_2:PtOEP film. This is in contrast to earlier work [55], where the dye was simply mixed into the sample solution. Furthermore, when the PS:TiO_2:PtOEP film is used without the deposited analyte, it was shown to be capable of O_2 gas sensing from 0 to 100% oxygen content.

Figure 5. Structurally integrated OLED sensor for loc sensing of oxygen, glucose, alcohol and lactate, with associated photoluminescence decay graphs. Figure re-used from Ref. [56] with permission, copyright 2008 Elsevier B. V.

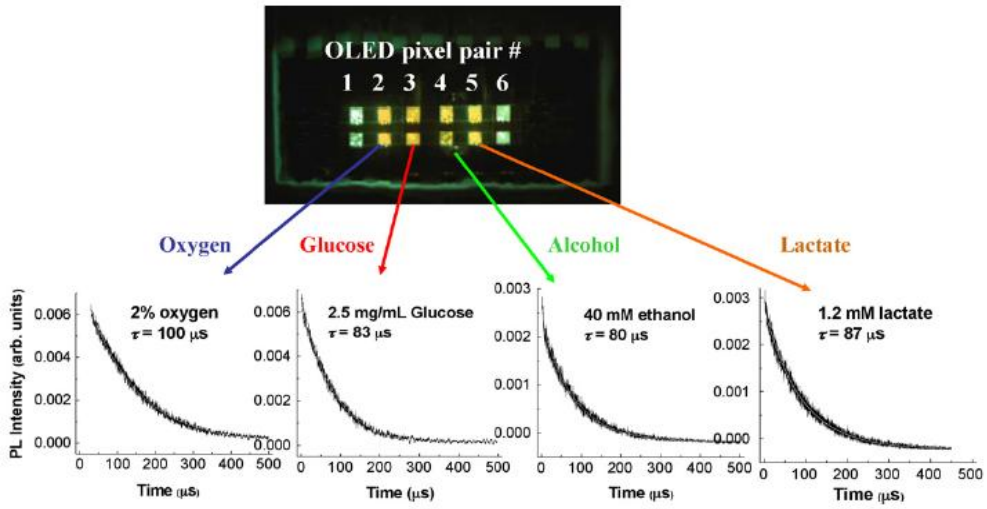

Edel *et al.* pursued a PL-sensing LoC with microchannels etched in glass and a spincoated, blue-emitting fluoropolymer OLED as an excitation source [66]. The authors used their microfluidic channels for electrophoretic separation of fluorescein and 5-carboxyfluorescein. The fluoropolymer was chosen so that its emission spectrum overlapped the absorption spectra of the fluorescein dyes at ~500 nm. Standard filters, lenses and a PMT or a Si APD were used for PL detection. The authors note that higher OLED driving voltages resulted in significantly larger SNRs, with a maximum SNR of 840 for a 10 mM 50 nL fluorescein plug. Detector intensities as well as separation times for the fluorescein dyes were comparable for the OLED excitation source *versus* a standard mercury lamp source.

Yao *et al.* used an NPB/Alq_3 bilayer OLED as an excitation source coupled with PDMS microchannels to measure PL from Rhodamine 6 g and Alexa Fluor 532 [69]. In this work, the researchers used an alternating layered TiO_2/SiO_2 DBR interference filter to block >555 nm light and thus to reduce the noise from the OLED excitation light. This allowed for a 13-times improvement in sensitivity of Rhodamine 6G dye. Yao and coworkers achieved SNR values of 16.9 and 10.2 using 50 μM Rhodamine 6G and 7 mM Alexa 532 respectively. The concentration limit for Alexa 532 was found to be 3 μM with a 0.7 nL injection volume. The researchers also applied their LoC system for separation of bovine serum albumin (BSA) conjugates.

In later work, Yao and coworkers used EL from a long-strip OLED for imaging fluorescently-labelled isoelectrically focused species [70]. This particular approach is a substantial

improvement over commercial techniques, which typically use a mobilization step to transport isoelectrically focused zones. This mobilization step is both time-consuming, and can cause smearing and distortion of the sample bands. While some attempts have been made to perform whole-column PL imaging with more traditional excitation sources [77,78], they generally suffered from non-uniform excitation. In contrast, an OLED can be fabricated adjacent to a linear microchannel with nearly any desired dimensions and relatively uniform emission. It is therefore a perfect candidate as a whole-channel excitation source. Using a CCD detector, the researchers isoelectrically focused R-phycoerythrin (finding 3 bands instead of 1 band due to impurities) within 30 s and note a system sensitivity of ~2.5 nM, as shown in Figure 6.

Figure 6. Isoelectric focusing electropherograms of *R*-phycoerythrin from an OLED-LoC system. (**A**) CCD intensity readout at varying concentrations in a 4-cm channel. (**B**) Time evolution of isoelectric focusing for 25 mg/mL in a 2 cm channel. Figures re-used from Ref. [70] with permission, copyright 2006 American Chemical Society.

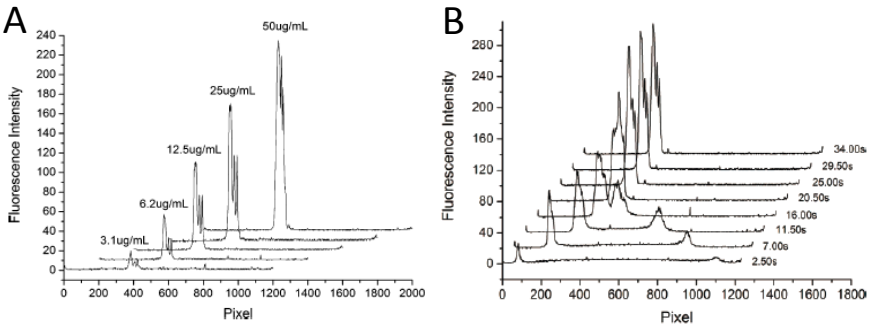

As an alternative approach to OLED-based detection of isoelectric focused species, Ren *et al.* of the same research group examined an active-matrix OLED pixel array as an excitation source [68]. In this manner, the resolution of the fluorescent image of the channel is determined by the size of each individual OLED pixel. In order to generate a full channel image, the pixels are addressed individually from one end of the array to the other. Fluorescent light from the labelled species can be measured by a simple photodiode and the photocurrent readings stitched together. This approach greatly relaxes the requirements of the detector. The researchers successfully applied this system to isoelectrically focus *R*-phycoerythrin to its isoelectric point within ~70–100 s.

Highlighting the need to miniaturize their entire LoC system, Shin and Kim *et al.* investigated a fully integrated microfluidic system with an Alq_3 OLED excitation source and a p-i-n Si PD [71,72]. The microchannel itself was etched in glass, and the OLED was deposited onto the same glass substrate. Shin *et al.* also employed an alternating SiO_2/TiO_2 interference filter on their p-i-n Si PD, and bonded the PD to the glass substrate. The authors compared the OLED to a laser source, and noted two orders of magnitude poorer PL from rhodamine 6G (by their PD photocurrent) due to excitation with the OLED. This was attributed to the poor OLED emission intensity. It is possible that higher brightness OLEDs could fare better for this LoC system, with state-of-the-art phosphorescent OLEDs granting substantially higher brightness and current efficiency values [79]. Regardless, Shin, Kim and coworkers demonstrated their LoCs to be capable of measuring 10 μM of tetramethylrhodamine and 1 μM of rhodamine 6G.

Following the above reasoning, Nakajima and coworkers studied a LoC system with a tris(2-phenylpyridine)iridium ($Ir(ppy)_3$) emitter, using the following OLED structure: ITO/*N*,*N*'-diphenyl-*N*,*N*'-di(m-tolyl)-benzidine (TPD)/4,4'-Di(*N*-carbazolyl)biphenyl (CBP):$Ir(ppy)_3$/4,7-diphenyl-1,10-pheranthoroline (Bphen)/Alq_3/Mg:Ag/Ag. This particular device structure employs an HTL, a guest:host EML and two ETLs, and ultimately allows for very high brightness values. As a first demonstration in a LoC system with a bandpass-filtered CCD detector, Nakajima and coworkers detected 7.8 mM resorufin flowing through PDMS microchannels. They further showed the system to be capable of detecting 16.5 ng/mL of immunoglobulin A (IgA) in an immunoassay experiment.

4.2. Organic Photodiode-Integrated Lab-on-a-Chip Systems

A summary of the LoC systems employing an OPD detector are provided in Table 2. Similar to Table 1, the results have been grouped together by their specific application, which coincides with the principal investigators. Also, for the cases where a dynamic range is not explicitly listed, values have been obtained from figures within the publications (best dynamic range noted for groups of publications).

Table 2. Summary of lab-on-a-chip systems with OPD detectors.

Application		Micro-fluidic	OPD Details	Excitation Source	Analyte	Dynamic Range	Ref.
H_2O_2/Anti-oxidant conc, TAC assay	CL CLq	PDMS channel	ITO/CuPc/C60/BCP/Al	N/A	H_2O_2	10 μM–1 M	[80–82]
					β-Carotene	22–200 μM	
			ITO/PEDOT:PSS/ P3HT:PCBM/Al		α-Tocopherol	10–200 μM	
					Quercetin	50–200 μM	
Dye conc	CL	PDMS channel	ITO/PEDOT:PSS/ CuPc/C60/LiF/Al	m-halide lamp w/ polarizer	Rh6g, fluorescein	10 nM–10 μM	[83]
Immuno assay	CL	PDMS channel	ITO/PEDOT:PSS/ P3HT:PCBM/Al	N/A	SEB	0.1–50 ng/mL	[84]
Light scattering, cell counting	abs	PDMS channel	P3HT:PCBM-based OPD (spraycoat)	488 nm laser	HeLa, NHDF, Jurkat cells	4E3–3E5 cells/cm^2	[85,86]
Multi-analyte conc	PLq abs	film, PDMS channel, pipette	Au/Moo3/CuPc/ PTCBI/Bphen/Ag	LEDs (various) w/ aperture	O_2, CO_2	0–20%	[87–91]
					pH	5–10	
					RIU	n = 1.33–1.43	
Dye conc, immuno assay	CL PL	PDMS channel	ITO/CuPc/ C_{60}/BCP/Al	LEDs (various) w/fibre	resorufin	1–50 μM	[92,93]
					IgA	20–120 ng/mL	
			ITO/CuPc/ CuPc:C60/ C_{60}/BCP/Al		APnEOs	2–50 ppb	
Immuno assay	CL	sol'n in wells, PDMS channel	ITO/PEDOT:PSS/ PCDTBT: PC70BM/LiF/Al	N/A	rhTSH	30 pg/mL–10 ng/mL	[94–97]
					human cortisol	0.28 - 249 nM	

Banerjee *et al.* studied the PL of rhodamine 6G and fluorescein using a PDMS microchannel, a halide lamp excitation source and a CuPc-C_{60} bilayer heterojunction OPD [83]. Their work focused on the ultimate limit of detection of a fully integrated LoC PL system, and thus highlighted the need to prevent excitation light from reaching the OPD. In a similar vein as Ryu *et al.* ([46]), Banerjee and coworkers used polarizers that were aligned orthogonal to each other and placed at the halide lamp and the OPD respectively. The OPD and its polarizer were bonded directly to the PDMS microchannel. By altering the orientation of the polarizer at the halide lamp from 0 °offset to 90 °offset, the authors noted a decrease in the OPD current (due to the excitation source background) from 5 μA to 19 nA. The dark current of the OPD on its own (with the excitation source off) was found to be 13 nA. This system allowed for detection of Rhodamine 6G at a concentration of 10nM.

Miyake and coworkers also examined LoC systems based on CuPc-C_{60} photodiodes [93]. Both bilayer and BHJ OPDs were fabricated with the device structures ITO/CuPc/C_{60}/bathocuproine (BCP) /Al and ITO/CuPc/CuPc:C_{60} (3:2)/C_{60}/BCP/Al respectively. Note that the latter BHJ device is in fact a PM-HJ OSC, which has neat donor and acceptor layers bordering the mixed donor:acceptor layer. The PM-HJ device architecture allows for enhanced absorption and free carrier transport properties due to the neat donor and acceptor layers, while granting efficient exciton separation within the mixed layer. In an optimized device structure, the neat donor and acceptor layer thicknesses are ideally chosen to be equal to the exciton diffusion lengths in the respective materials. The researchers completed their LoC PL detection system by placing a green LED below their PDMS microchannels, and their OPD above the microchannels. In order to minimize excitation light coupled into the OPD, Miyake *et al.* made use of a bandpass filter (in lieu of the polarizers used by Banerjee *et al.* [83]), granting a limit of detection of 1 mM resorufin. They further employed their LoC system in an immunoassay to detect 20 ng/mL IgA. Continuing this work, Ishimatsu *et al.* performed competitive ELISA of alkylphenol polyethoxylates (APnEOs) on magnetic microbeads in PDMS microchannels [92]. To this end, the researchers used a magnet to immobilize anti-APnEO-immobilized beads within the microchannel, and subsequently flowed APnEOs and the secondary sensing antibodies through the same microchannel. Their results showed an APnEO limit of detection of 2 ppb.

Hofmann *et al.* similarly examined OPD-microfluidic systems based on both planar heterojunction and BHJ CuPc-C_{60} photodiodes [80]. These OPDs were fabricated on glass substrates and were subsequently bonded to PDMS microchannels. Using their bilayer CuPc/C_{60} OPD, the researchers achieved peak external quantum efficiencies (EQEs) of ~25%–30% at wavelengths near 600–700 nm. Hofmann and coworkers also found a strong limitation to the ultimate limit of detection (LoD) of their system to be due to their OPD's absorption of excitation light. The researchers later developed long-pass thin-film filters based on doping PDMS with lysochrome dyes [98]. The use of PDMS and common biochemical dyes make these filters especially attractive, as they are easily compatible with standard microfluidics fabrication. As a first verification of the capabilities of their integrated OPD-microchannel device, Hofmann *et al.* measured peroxyoxalate chemiluminescence (CL). Both bis (2-carbopentyloxy-3,5,6-trichlorophenyl) oxalate (CPPO) and 9,10-diphenylanthracene dye were introduced into a first sample well, H_2O_2 was introduced into a second sample well and 4-dimethylaminopyridine (DMAP, catalyst) was introduced into a third sample well. The three species were hydrodynamically pumped to meet at a channel intersection and then mixed along a 1-cm-long

linear segment. The authors noted a limit of detection of ~1 mM H_2O_2, and they observed a linear relationship of the OPD current with the H_2O_2 concentration up to 1 M.

Wang and coworkers of the same research group studied a similar LoC system, but instead used a P3HT:PCBM-based OPD [82]. Their OPD device structure was ITO/poly(3,4-ethylenedioxythiophene) poly(styrenesulfonate) (PEDOT:PSS)/P3HT:PCBM (1:1)/Al. As noted previously, P3HT:PCBM absorbs over most of the visible range (~350m to 700nm), and so this particular OPD would not be applicable to LoC systems that require absorption over a small bandwidth (e.g., LoC systems with several OPDs to detect multiple PL peaks). In this work, the researchers patterned and miniaturized their OPDs to better align with the geometry of their microchannels to decrease dark current. As a consequence, using a similar CL reaction as described with [80], Wang *et al.* were able to achieve an H_2O_2 limit of detection less than 10 μM, with linear OPD photocurrent *vs.* concentration until 1 mM H_2O_2. This level of sensitivity is on par with a similar system using an integrated silicon photodiode [99]. Wang *et al.* later applied their P3HT:PCBM OPD-LoC for the evaluation of the antioxidant capabilities of β-carotene, α-tocopherol and quercetin, granting detection limits 10–50 μM [81]. The researchers compared the transient OPD signal to the same system using a PMT detector. They found virtually identical signal profiles for the OPD *versus* the PMT detector, with nearly the same detection limits and precision. This work is therefore a strong evidence for the capability of integrated OPDs to replace the lab-scale detector set-ups in PL/CL measurements.

Wojciechowski *et al.* applied a P3HT:PCBM OPD to detect CL from sandwich immunoassays for detection of Staphylococcal enterotoxin B (SEB) [84]. Similar to the work by Wang *et al.*, the authors note very low (pA) dark currents with fA noise for their P3HT:PCBM OPDs when kept under low reverse bias (0 to 100 mV). OPDs were fabricated on glass substrates, and attachment and assay steps were simply completed on the reverse side of the substrates with a patterned PDMS reservoir. The samples were then fitted with a microfluidic flow chamber and inserted into a custom-made hand-held controller. The components of this system are shown in Figure 7. Their efforts allowed for a limit of detection of 0.5 ng/mL SEB, which is on par with commercially available 'portable' PMT-based and CCD-based systems. Furthermore, while these commercially available systems tout portability, they are substantially heavier and costlier than the presently examined OPD-LoC system.

Figure 7. Various components of the hand-held OPD PL measurement system by Wojciechowski *et al.* (**A**) From left to right: PMMA holder, PDMS reservoir, glass sensor slide with OPD, opaque microfluidic channel. (**B**) hand-held controller. Figure re-used from Ref. [84] with permission, copyright 2009 American Chemical Society.

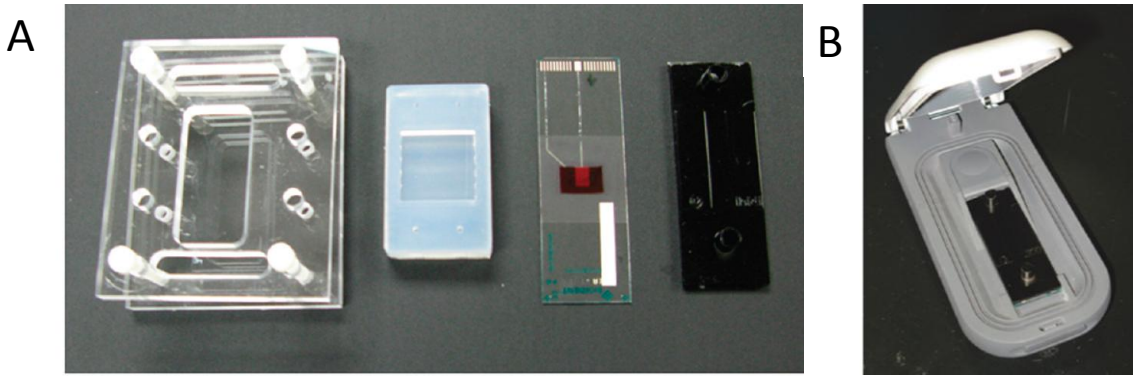

Following the shift in the organic photovoltaics community toward new donor polymers and C_{70}-fullerene derivatives (instead of the more common $PC_{60}BM$), Pires *et al.* studied BHJ OPDs based on a poly [*N*-9'-heptadecanyl-2,7-carbazole-alt-5,5-(4',7'-di-2-thienyl-2',1',3'-benzothiadiazole)] (PCDTBT) donor and a [6,6]-phenyl C71-butyric acid methyl ester ($PC_{71}BM$) acceptor for their LoC systems [94–97]. Such OPDs have been shown to be capable of very high efficiencies [100], and internal quantum efficiencies approaching 100% over a large portion of the visible spectrum [101]. They are thus ideal candidates for LoC systems, where the PL from dilute analyte can be quite weak. The OPD integrated with either micro-wells or PDMS microchannels allowed for detection of CL from 30 pg/mL of recombinant human thyroid stimulating hormone (rhTSH) and 0.28 nM of human cortisol. Pires *et al.* also showed that the PCDTBT:$PC_{71}BM$ OPDs could be used with PMMA microchannels for multiplexed detection of pathogens [97], with the total cost of their detection system estimated at less than $30 USD.

In order to demonstrate the versatility of integrated OPD-LoC technology, Lamprecht, Abel, Sagmeister and coworkers fabricated a number of different multi-analyte sensors to pair with bilayer CuPc/PTCBI OPD detectors [87–91]. Similar to the work by Shinar and coworkers [55–57,65], O_2 gas concentration is measured by PL quenching (PLq) of films that employ O_2-sensitive phosphorescent materials (e.g. (II) meso-tetra(pentafluorophenyl)porphine (PtTFPP)). This is accomplished by exciting the sensing film with an LED and detecting the change in PL intensity and PL decay dynamics with changing O_2 concentration—the PtTFPP triplet state is generally long-lived but prone to quenching by O_2. CO_2 and pH were also shown to be measurable by changing the sensing film to films based on either 8-hydroxypyrene-1,3,6-trisulfonic acid trisodium salt (HPTS):tetra-*N*-octylammonium hydroxide (TOA^+OH^-) or $HTPS(DHA)_3$ respectively. In order to reduce dark noise and improve the sensitivity of their LoC systems, the researchers employ a unique system geometry with ring-shaped OPDs, as shown in Figure 8. This is an extension of the back-detection LoC geometry discussed previously; however, this system further decouples the excitation source and the detector by waveguiding the sensor film's PL to a ring-shaped OPD. To further enhance light coupling to the OPD in this geometry, the researchers also used a scattering ring opposite to the OPD. The use of waveguided light also opens up possibility for surface plasmon resonance test platforms, where the sensor spot is replaced by Ag/Ta_2O_5 thin films. Evanescent waves that penetrate the cladding of the waveguide interact with analyte adjacent to the SPR platform, which can then be detected by the OPD. Lamprecht *et al.* employed such a system to test for changes in refractive index in adjacent fluid, allowing for the detection of changes in refractive index with a resolution of 8E-4 RIU. This resolution is on par with similar systems developed by Ratcliff *et al.*, which make use of Alq_3/TPD OLED emitters and double pentacene/C_{60} detectors [102].

In their most recent work, Lamprecht *et al.* adapted this same LoC test platform to a glass pipette, placing the sensor film material within the pipette, and then depositing the OPD around the edge of the pipette away from the sensor spot [89]. In this case, the glass walls of the pipette act as the waveguide. This particular application highlights the promise of organic electronic materials and devices in LoC systems. Specifically, OPDs and OLEDs are incredibly adaptable—they are capable of being deposited on many different substrates at low temperatures, including substrates that are flexible and non-planar.

Figure 8. Illustration of the loc system employing a ring-shaped OPD for Reduced dark noise. Figure re-used from Ref. [91] with permission, copyright 2013 Springer.

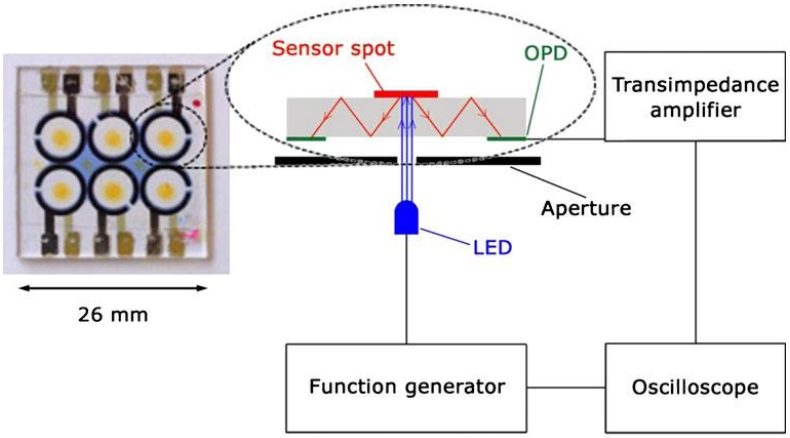

4.3. Fully Integrated OLED/OPD Lab-on-a-Chip Systems

A summary of the LoC systems employing both an OLED excitation source and an OPD detector are provided in Table 3. As with the previous tables, the results have been grouped together by their specific application, which coincides with the principal investigators. Also, for the cases where a dynamic range is not explicitly listed, values have been obtained from figures within the publications (the best dynamic range is noted for groups of publications). Furthermore, while the entries in Table 3 and the discussion below primarily focus on experimental OLED-OPD-LoC systems, it is worth noting that some work has been done on modelling these systems to extract ultimate limits of detection [103,104].

Table 3. Summary of lab-on–a-chip systems with OLED excitation sources and OPD detectors.

Application		Micro-fluidic	Excitation Source	Detector Details	Analyte	Dynamic Range	Ref.
Dye conc	PL	PDMS channel	ITO/EB390/NPB/ Alq3/LiF/Al	ITO/PEDOT: PSS/CuPc/C60/ LiF/Al	Rh6G	0.1 nM–1 mM	[105–108]
					fluor-escein	1 µM–1 mM	
Multi-analyte conc	PLq	film (non-MF)	Au/CuPc/NPB/ Alq3/LiF/Ag	Au/CuPc/ PTCBI/Alq3/ Ag	O2	0–20%	[109,110]
			Blue-emitting OLEDs		CO2	0–10%	
					pH	3–9	
Multi-analyte conc	PLq	film (non-MF)	ITO/CuPc/NPD/ Alq3:C545T/ Alq3/LiF/Al	ITO/PEDOT: PSS/P3HT: PCBM/Al	O2	0–100%	[111,112]
			Ag/MoO3/α-NPB/Alq3/LiF/Al	ITO/LiF/CuPc/ C70/Bphen/Al	pH	4–10	
Cell counting, herbicide conc	PL	PDMS channel	ITO/NPB/DPVBi/ BCP/Alq3/LiF/Al	ITO/PTB3: PCBM/LiF/Al	green algae CC-125	2.1E5–3E6 cells/mL	[113]
					DCMU	7.5 nM–1.5 µM	
Immuno assay, Spectro-scopy	abs	PMMA + tape	ITO/PEDOT:PSS/ Ir(mppy)3:PVK :TPD:PBD/Ba/Al	ITO/P3HT: PCBM/Ba/Al w/ etched glass grating	mIgG	N/A	[114]

Banerjee, Pais and coworkers continued their earlier work by replacing their halide lamp excitation source with a green-emitting Alq_3 OLED [105–107]. As with their previous experiments discussed in Section 4.2, the researchers made use of a CuPc-C_{60} bilayer heterojunction OPD as a detector. The authors noted an increase in the limit of detection for rhodamine 6G from 10 nM to 100 nM when switching from the halide lamp to the OLED. The authors also measured a limit of detection of 10 μM fluorescein for their system—much higher than that of rhodamine 6G due to the poor spectral overlap of fluorescein with the Alq_3 OLED and the poorer OPD responsivity at ~530 nm (where fluorescein emits light). The authors note that with optimization of channel depth, OPD responsivity and OLED output power, a detection limit of 10 pM should be feasible. By further reducing the noise within the associated system electronics (including connecting wires, the lock-in amplifier, the multimeter and the GPIB-USB connector), even lower detection limits are possible.

Shuai *et al.* of the same research group later improved upon this fully integrated system, replacing the simple bilayer heterojunction OPD with a multiple heterojunction OPD [108]. Both an illustration and a photograph of their experimental setup are shown in Figure 9. The multiple heterojunction OPD is discussed at depth in [11], and uses multiple thin absorbing layers to increase the OPD absorption. If the device is designed correctly, such that the layer thicknesses are smaller than the respective exciton diffusion lengths, the multiple heterojunction can strongly enhance OPD quantum efficiency. Their final OPD device structure is thus ITO/PEDOT:PSS (HIL/HTL)/CuPc (HTL)/C_{60} (ETL)/CuPc (HTL)/C_{60} (ETL)/LiF (EIL)/Al. By using this improved OPD with polarizers to reduce dark noise, the researchers lowered their limit of detection for rhodamine 6G to 1 nM.

Figure 9. Illustration and photograph of a fully integrated organic light emitting diode-organic photodetector-lab-on-a-chip PL detection system. Figure re-used from Ref. [108] with permission, copyright 2008 IEEE.

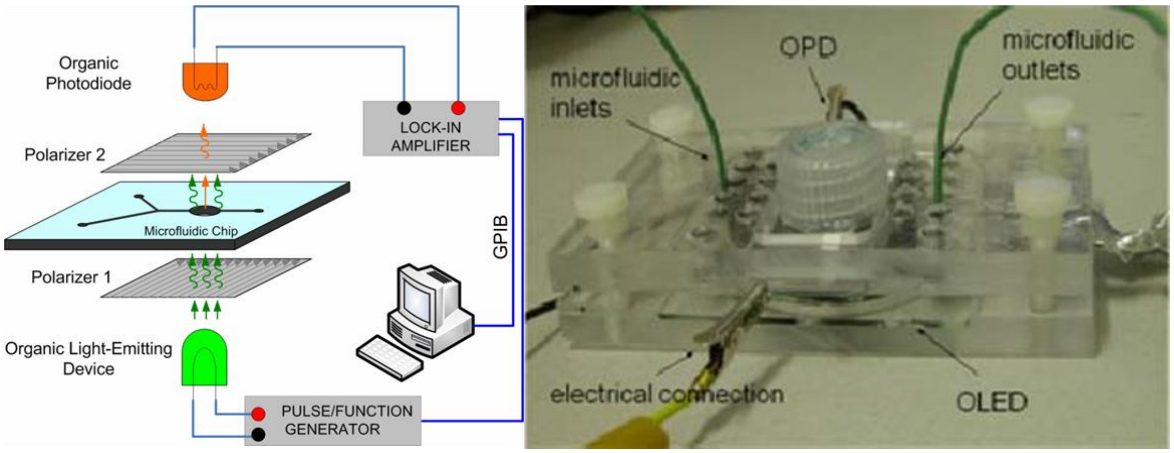

Kraker and coworkers also made use of an Alq_3-based OLED and a CuPc-PTCBI OPD with polarizers [109], applying this PL detection scheme to their O_2-sensitive films (detailed in Section 4.2 with Sagmeister, Lamprecht, Abel *et al.* [87–91]). In order to prevent OLED excitation light from reaching the OPD, both the OLED and OPD were fabricated directly on the polarizer foils. A PtTFPP:PS film was then deposited on the reverse-side of the OLED foil for efficient measurement of oxygen content. The authors further employed this system as a pH sensor using fluorescein-isothiocyanate in phosphate buffer. Since organic electronics can be readily deposited on flexible substrates

(including polarizer foils), this approach highlights a feasible, and potentially cost/time-saving improvement to the LoC fabrication process. Mayr *et al.* of the same research group instead used blue emitting OLEDs in combination with a CuPc-PTCBI OPD to detect O_2 and CO_2 gas concentrations [110]. Here the authors employ the ring-OPD geometry described earlier (shown in Figure 8), to detect 0 to 20% O_2, 0 to 10% CO_2 and 3 to 9 pH with a fast and reversible sensor response. The response of the fully integrated LoC with all-organic optical detection is thus shown to be on par with their previous LoCs, which used inorganic LED excitation sources.

Nalwa, Liu and *et al.* also examined OLED-OPD-LoC systems for O_2 and pH sensing [111,112], continuing the progress on multi-analyte detection with Shinar and coworkers. Nalwa *et al.* employed a coumarin 545T (C545T)-doped Alq_3 fluorescent OLED as an excitation source and a longpass-filtered P3HT:PCBM OPD for PL detection [112]. The work allowed for the detection of 0 to 16% O_2. As such, this system is also capable of similar performance as previously studied LoCs that used inorganic PMT, CCD or Si PD detectors. The combination of this research with that of Kraker *et al.* noted above thus shows that completely organic optical detection for LoC is a practical alternative to more common inorganic detection schemes from both the perspective of the excitation source and the detector. Liu *et al.* focused on further optimizing the sensitivity of their multi-analyte LoCs by addressing the generally large full-width at half-maximum (FWHM) of OLED electroluminescence [111]. To this end, the researchers employed microcavity OLEDs and the back-detection system geometry to substantially reduce the dark noise of their LoC systems by reducing the OLED light detected by their OPD. In this work, the OLED has the following structure: Ag/MoO3/α-NPD/Alq_3/LiF/Al, with the silver layer deposited to only 40 nm to remain semi-transparent to the Alq_3-emitted light. By fine-tuning the thicknesses of the α-NPD and Alq_3 layers, Liu *et al.* showed it was possible to use constructive/deconstructive interference to change the color of their microcavity OLEDs from green to blue. Longpass-filtered CuPc/C_{70} bilayer OPDs were used due to their strong EQE overlap with their PtOEP-based sensing layer absorption. By measuring the PL decay dynamics of PtOEP-based films and the PL intensity variations of solutions containing fluorescein, the researchers achieved sensing of 0 to 100% O_2 and 4 to 10 pH respectively.

Lefèvre *et al.* examined a fully integrated OLED-OPD-LoC system for detection of algal chlorophyll [113]. Chlorophyll complex molecules in photosystem II use absorbed energy for photosynthesis, which can be generated from blue photons, and subsequently re-emit excess energy in the far red region. This system is particularly interesting for LoC PL detection, as the absorption and emission bands are spaced ~200 nm apart. The researchers used a blue DPVBi-based OLED for excitation and a polymeric PTB3:PCBM BHJ OPD for detection. The PTB class of polymers was developed for OSCs, and has been shown to yield solar cells with very high performance [115,116]. It is based on alternating ester substituted thieno[3,4-*b*]thiophene and benzodithiophene units and exhibits an absorption peak at 700 nm, with tail-end absorption extending up to 800 nm. It is thus ideal for the present application, as it can absorb the far-red photons emitted by algal chlorophyll. To further minimize dark noise due to OLED light being detected by the OPD, Lefèvre and coworkers used thin-film filters formed by incorporating dyes into host resin. In fact, the ease of implementation and success of these thin-film absorbing filters follows as a consequence of the large separation between the OLED EL peak and the chlorophyll PL peak. Both the OLED and the OPD were formed on glass substrates and subsequently bonded back-to-back to the PDMS microchannels with their relevant

filters. An illustration and photograph of the system layout are shown in Figure 10. Lefèvre *et al.* used this system to identify a limit of detection of ~1900 algal cells within their detection chamber (2.1E5 cells/mL). The researchers further used this system for detection and quantitation of herbicides, with Diuron (DCMU) concentrations as low as 7.5 nM, surpassing the detection limit of portable commercial equipment by an order of magnitude.

Figure 10. (**A**/**B**) Illustration of a fully integrated organic light emitting diode(OLED)-organic photodetector(OPD)-lab-on-a-chip PL detection system. (**A**/**B**) (**a**) OPD (**b**) excitation filter (**c**) microfluidic channels (**d**) emission filter (**e**) OLED. (**C**) photograph of the microchannels (colour dyes show channels). Figure re-used from Ref. [113] with permission of The Royal Society of Chemistry.

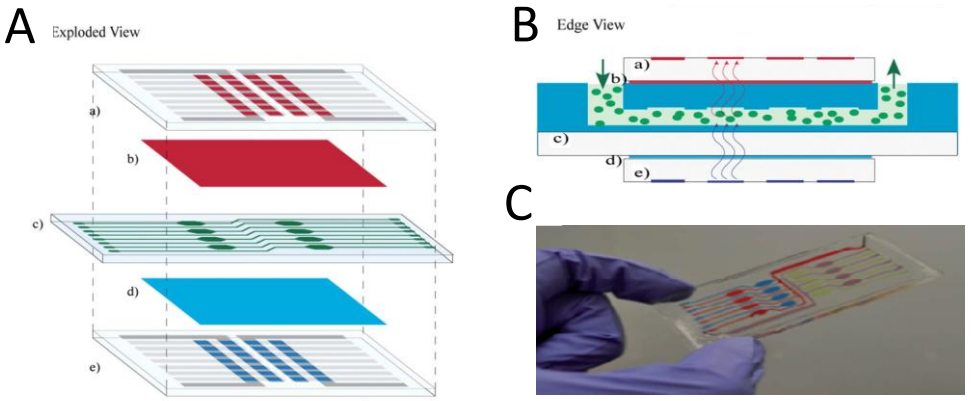

As a final demonstration of the potential for fully integrated organic electronic optical detection schemes for LoC applications, we examine work completed by Ramuz, Leuenberger and Bürgi, who used polymer OLED emitters and OPD spectrometers for flow immunoassays [114]. Their system relies on SPR interaction with analyte in PMMA microchannels by using a $SiO_2/TiO_2/Cr/Au/TiO_2$ SPR sensing platform, with the specific LoC geometry shown in Figure 11. The researchers employed a phosphorescent polymer OLED with the structure ITO/PEDOT:PSS/ tris[2-(*p*-tolyl)pyridine]iridium(III) ($Ir(mppy)_3$):poly(9-vinylcarbazole) (PVK):TPD:PBD/Ba/Al. The polymer LED pumps a 'PL-material', MEH-PPV, to efficiently couple excitation light into the waveguide. The indirect excitation with the MEH-PPV 'PL-material' provides better TM mode coupling into the waveguide when compared to direct excitation of the polymer OLED. The second benefit to this method is that the intensity of the light coupled into the waveguide can be scaled with the size of the MEH-PPV PL layer and the size of the polymer OLED. After passing the SPR platform, the waveguided light propagates to a 500 μm grating of etched glass (312 nm period, 12 nm depth), which scatters light into an OPD array (10–50 μm-wide OPD pixels with 5 μm pitch. This approach impressively acts as a spectrometer with 5 nm resolution. Using this system, Ramuz *et al.* performed an immunoassay for mouse immunoglobulin G (mIgG). Spectra during each stage of the immunoassay were obtained, and clear changes were observed for both the functionalization of the microchannel with mIgG, as well as the subsequent addition of anti-mIgG labelled with the Cy5 fluorescent marker. While this initial demonstration is already impressive, the incorporation of a fully functional organic

spectrometer into LoC has incredible potential, and can be easily applied to any number of optical bio-detection experiments.

Figure 11. Illustration of a LoC system using SPR-absorption analyte detection with a polymer OLED excitation source and an OPD spectrometer. Figure re-used from Ref. [114] with permission, copyright 2010 Wiley Periodicals, Inc.

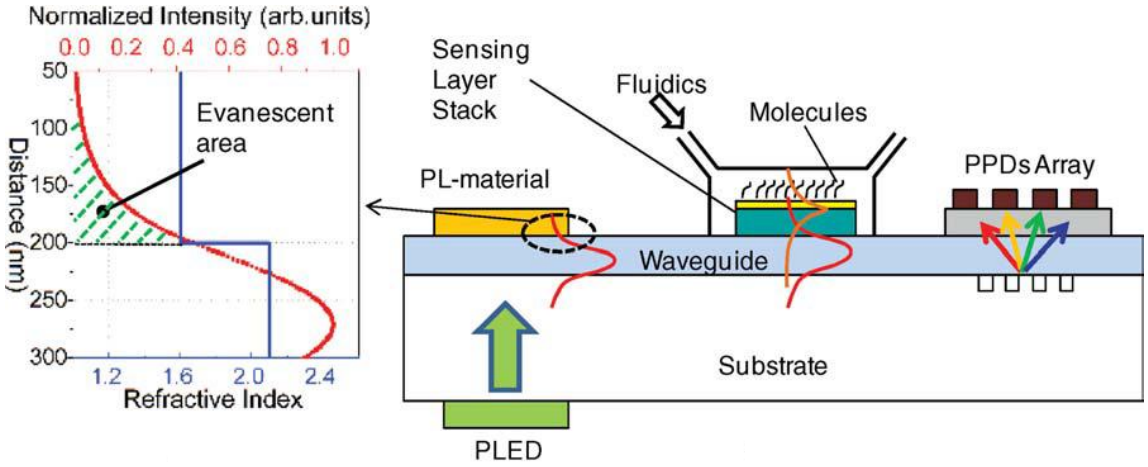

5. Conclusions

LoC systems promise substantial improvements in many analytical procedures, especially in those implementing complicated lab-based techniques to simple point-of-care tests. However, LoC systems also suffer in that they are inherently multidisciplinary endeavours, requiring expertise in incredibly varied fields of study. The present review examined the meshing of three core fields of research—organic electronics, microfluidics and life sciences. The entrance difficulty associated with application of all of these fields simultaneously has resulted in a relatively under-developed area of study. To this end, there are only a handful of examples of truly integrated PL LoC systems that do not require external lab space and equipment. In spite of this, the preliminary data from the reviewed research overwhelmingly supports the fact that optimized OLED-OPV-LoC PL systems are certainly capable of surpassing current commercial portable analysis technology, and in some cases may even rival lab-scale set-ups.

Arguably the most critically important parameter to dictate a PL system's realm of applicability is its limit of detection. In most studies, researchers identified the detector's absorption of the excitation light as a hindrance to the limit of detection, since it increases the background or zero-point signal. In lab-scale set-ups, the majority of excitation light can be removed by clever placement of the detector—ideally orthogonal to the excitation source and 45 ° to the channel. In a scaled down LoC system, this geometry is unwieldy and difficult to implement. As such, researchers have pursued back-detection architectures, waveguide-coupled PL, time-delayed and PL lifetime analysis, interference filters, absorbing filters and polarizer films to varying degrees of success.

The other most significant impediments to the ultimate limit of detection are related to the quality of the OLED and OPD. Namely, most research on this topic to date can be best described as proof-of-concept, using the simplest bilayer Alq_3 OLEDs and the most basic CuPc-C_{60} or P3HT:PCBM OPDs. These studies have done well to invigorate and spur new research—the past

decade of research has allowed for applications of this technology spanning simple chemical detection, to imaging whole-channel isoelectric focusing, to observing peroxyoxalate CL, to miniaturized organic spectrometers and finally to the measurement of algal PL for herbicide characterization. However, as noted by Banerjee and coworkers [105], the output power of their OLED must be improved by up to 150-times and the responsivity of their OPD must be improved by up to 50-times for their integrated LoC system to reach lab-scale sensitivities. Other improvements can be made in LoC system geometry, as has been observed with the successful use of ring-OPDs and OPDs deposited on circular substrates. It is now necessary to push the OLED-OPV-LoC system to its limits to probe its ultimate capabilities.

Acknowledgments

Financial support to this work from the Natural Sciences and Engineering Research Council of Canada (NSERC) is gratefully acknowledged. GW acknowledges financial support through NSERC Alexander Graham Bell Canada Graduate Scholarship, Ontario Graduate Scholarship, and WIN Nanofellowship.

Conflicts of Interest

The authors declare no conflict of interest.

References

1. Roman, G.T.; Kennedy, R.T. Fully integrated microfluidic separations systems for biochemical analysis. *J. Chromatogr. A* **2007**, *1168*, 170–188.
2. Yi, C.; Li, C.W.; Ji, S.; Yang, M. Microfluidics technology for manipulation and analysis of biological cells. *Anal. Chim. Acta* **2006**, *560*, 1–23.
3. Haeberle, S.; Zengerle, R. Microfluidic platforms for lab-on-a-chip applications. *Lab Chip* **2007**, *7*, 1094–1110.
4. Kajiyama, Y.; Joseph, K.; Kajiyama, K.; Kudo, S.; Aziz, H. Recent Progress on the Vacuum Deposition of OLEDS with Feature Sizes ≤ 20 μm Using a Contact Shadow Mask Patterned in-situ by Laser Ablation. In *Organic Light Emitting Materials and Devices XVII*, Proceedings of SPIE 8829, San Diego, CA, USA, 25 August 2013; So, F., Adachi, C., Eds.; SPIE International Society for Optical Engineering: Bellingham, WA, USA; p. 882919.
5. Kajiyama, Y.; Wang, Q.; Kajiyama, K.; Kudo, S.; Aziz, H. Vacuum Deposition of OLEDS with Feature Sizes ≤ 20um Using a Contact Shadow Mask Patterned in-situ by Laser Ablation. In *Proceeding of SID Symposium Digest of Technical Papers*, 2012; Wiley Online Library: Hoboken, NJ, USA, 1 October 2012; pp. 1544–1547.
6. Mishra, A.; Bäuerle, P. Small molecule organic semiconductors on the move: Promises for future solar energy technology. *Angew. Chem. Int. Edit.* **2012**, *51*, 2020–2067.
7. Mas-Torrent, M.; Rovira, C. Novel small molecules for organic field-effect transistors: Towards processability and high performance. *Chem. Soc. Rev.* **2008**, *37*, 827–838.

8. Duan, L.; Hou, L.; Lee, T.-W.; Qiao, J.; Zhang, D.; Dong, G.; Wang, L.; Qiu, Y. Solution processable small molecules for organic light-emitting diodes. *J. Mater. Chem.* **2010**, *20*, 6392–6407.
9. Tang, C.; VanSlyke, S. Organic electroluminescent diodes. *Appl. Phys. Lett.* **1987**, *51*, 913–915.
10. Van Slyke, S.; Chen, C.; Tang, C. Organic electroluminescent devices with improved stability. *Appl. Phys. Lett.* **1996**, *69*, 2160.
11. Peumans, P.; Yakimov, A.; Forrest, S.R. Small molecular weight organic thin-film photodetectors and solar cells. *J. Appl. Phys.* **2003**, *93*, 3693–3723.
12. Pohl, R.; Montes, V.A.; Shinar, J.; Anzenbacher Jr, P. Red-green-blue emission from tris (5-aryl-8-quinolinolate) al (iii) complexes. *J. Org. Chem.* **2004**, *69*, 1723–1725.
13. Inganäs, O.; Roman, L.S.; Zhang, F.; Johansson, D.; Andersson, M.; Hummelen, J. Recent progress in thin film organic photodiodes. *Synth. Met.* **2001**, *121*, 1525–1528.
14. Reyes-Reyes, M.; Kim, K.; Carroll, D.L. High-efficiency photovoltaic devices based on annealed poly(3-hexylthiophene) and 1-(3-methoxycarbonyl)-propyl-1-phenyl-(6,6)c-61 blends. *Appl. Phys. Lett.* **2005**, *87*, 083506.
15. Williams, G.; Wang, Q.; Aziz, H. The photo-stability of polymer solar cells: Contact photo-degradation and the benefits of interfacial layers. *Adv. Funct. Mater.* **2012**, *23*, 2239–2247.
16. Williams, G.; Aziz, H. In *Insights into Electron and Hole Extraction Layers for Upright and Inverted Vacuum-Deposited Small Molecule Organic Solar Cells*, Proceeding of Organic Photovoltaics XIV, San Diego, CA, USA, 17 October 2013; SPIE International Society for Optical Engineering: Bellingham, WA, USA, 2013; p. 88301.
17. Williams, G.; Aziz, H. The effect of charge extraction layers on the photo-stability of vacuum-deposited *versus* solution-coated organic solar cells. *Org. Electron.* **2013**, *15*, 47–56.
18. Xue, J.G.; Uchida, S.; Rand, B.P.; Forrest, S.R. Asymmetric tandem organic photovoltaic cells with hybrid planar-mixed molecular heterojunctions. *Appl. Phys. Lett.* **2004**, *85*, 5757–5759.
19. Ratcliff, E.L.; Garcia, A.; Paniagua, S.A.; Cowan, S.R.; Giordano, A.J.; Ginley, D.S.; Marder, S.R.; Berry, J.J.; Olson, D.C. Investigating the influence of interfacial contact properties on open circuit voltages in organic photovoltaic performance: Work function *versus* selectivity. *Adv. Energy Mater.* **2013**, *3*, 647–656.
20. Reineke, S.; Baldo, M.A. Recent progress in the understanding of exciton dynamics within phosphorescent oleds. *Phys. Status Solidi* **2012**, *209*, 2341–2353.
21. Birnstock, J.; Lux, A.; Ammann, M.; Wellmann, P.; Hofmann, M.; Stübinger, T. 64.4: Novel Materials and Structures for Highly-Efficient, Temperature-Stable, and Long-Living am OLED Displays. *SIDInt. Symp. Dig. Tech. Pap.* **2006**, *37*, 1866–1869.
22. Uhrich, C.L.; Schwartz, G.; Maennig, B.; Gnehr, W.M.; Sonntag, S.; Erfurth, O.; Wollrab, E.; Walzer, K.; Foerster, J.; Weiss, A. In *Efficient and Long-Term Stable Organic Vacuum Deposited Tandem Solar Cells*, Proceedings of SPIE Photonics Europe, Brussels, Belgium, 19 May 2010; International Society for Optics and Photonics: Bellingham, WA, USA, 2010, p. 77220G.
23. Figeys, D.; Pinto, D. Lab-on-a-chip: A revolution in biological and medical sciences. *Anal. Chem.* **2000**, *72*, 330–335.
24. Abgrall, P.; Gue, A. Lab-on-chip technologies: Making a microfluidic network and coupling it into a complete microsystem—A review. *J. Micromech. Microeng.* **2007**, *17*, R15.

25. Mark, D.; Haeberle, S.; Roth, G.; Von Stetten, F.; Zengerle, R. Microfluidic lab-on-a-chip platforms: Requirements, characteristics and applications. *Chem. Soc. Rev.* **2010**, *39*, 1153–1182.
26. Erickson, D.; Li, D. Integrated microfluidic devices. *Anal. Chim. Acta* **2004**, *507*, 11–26.
27. Hunt, H.C.; Wilkinson, J.S. Optofluidic integration for microanalysis. *Microfluid. Nanofluid.* **2008**, *4*, 53–79.
28. Liu, R.; Ishimatsu, R.; Nakano, K.; Imato, T. Optical sensing systems suitable for flow analysis on microchips. *J. Flow Injection Anal.* **2013**, *30*, 15–20.
29. Capitán-Vallvey, L.F.; Palma, A.J. Recent developments in handheld and portable optosensing—A review. *Anal. Chim. Acta* **2011**, *696*, 27–46.
30. Gai, H.; Li, Y.; Yeung, E.S. Optical Detection Systems on Microfluidic Chips. In *Microfluidics*, Springer: Heidelberg, Germany, 2011; pp. 171–201.
31. Yu, L.; Shen, Z.; Mo, J.; Dong, X.; Qin, J.; Lin, B. Microfluidic chip-based cell electrophoresis with multipoint laser-induced fluorescence detection system. *Electrophoresis* **2007**, *28*, 4741–4747.
32. Fu, J.L.; Fang, Q.; Zhang, T.; Jin, X.H.; Fang, Z.L. Laser-induced fluorescence detection system for microfluidic chips based on an orthogonal optical arrangement. *Anal. Chem.* **2006**, *78*, 3827–3834.
33. Irawan, R.; Tjin, S.C.; Fang, X.; Fu, C.Y. Integration of optical fiber light guide, fluorescence detection system, and multichannel disposable microfluidic chip. *Biomed. Microdevices* **2007**, *9*, 413–419.
34. Gao, J.; Yin, X.F.; Fang, Z.L. Integration of single cell injection, cell lysis, separation and detection of intracellular constituents on a microfluidic chip. *Lab Chip* **2003**, *4*, 47–52.
35. Roulet, J.C.; Völkel, R.; Herzig, H.P.; Verpoorte, E.; de Rooij, N.F.; Dändliker, R. Performance of an integrated microoptical system for fluorescence detection in microfluidic systems. *Anal. Chem.* **2002**, *74*, 3400–3407.
36. Bliss, C.L.; McMullin, J.N.; Backhouse, C.J. Integrated wavelength-selective optical waveguides for microfluidic-based laser-induced fluorescence detection. *Lab Chip* **2008**, *8*, 143–151.
37. Monat, C.; Domachuk, P.; Eggleton, B. Integrated optofluidics: A new river of light. *Nat. Photonics* **2007**, *1*, 106–114.
38. Schmidt, H.; Hawkins, A.R. The photonic integration of non-solid media using optofluidics. *Nat. Photonics* **2011**, *5*, 598–604.
39. Gersborg-Hansen, M.; Kristensen, A. Tunability of optofluidic distributed feedback dye lasers. *Opt. Express* **2007**, *15*, 137–142.
40. Chabinyc, M.L.; Chiu, D.T.; McDonald, J.C.; Stroock, A.D.; Christian, J.F.; Karger, A.M.; Whitesides, G.M. An integrated fluorescence detection system in poly (dimethylsiloxane) for microfluidic applications. *Anal. Chem.***2001**, *73*, 4491–4498.
41. Irawan, R.; Chuan, T.S.; Yaw, F.C. Integration of a fluorescence detection system and a laminate-based disposable microfluidic chip. *Microw. Opt. Technol. Lett.* **2005**, *45*, 456–460.
42. Irawan, R.; Tjin, S.C. Detection of fluorescence generated in microfluidic channel using in-fiber grooves and in-fiber microchannel sensors. *Meth. Mol. Biol.* **2009**, *503*, 403.
43. Seo, J.; Lee, L.P. Disposable integrated microfluidics with self-aligned planar microlenses. *Sensor. Actuat. B* **2004**, *99*, 615–622.

44. Mazurczyk, R.; Vieillard, J.; Bouchard, A.; Hannes, B.; Krawczyk, S. A novel concept of the integrated fluorescence detection system and its application in a lab-on-a-chip microdevice. *Sensor. Actuat. B* **2006**, *118*, 11–19.
45. Novak, L.; Neuzil, P.; Pipper, J.; Zhang, Y.; Lee, S. An integrated fluorescence detection system for lab-on-a-chip applications. *Lab Chip* **2007**, *7*, 27–29.
46. Ryu, G.; Huang, J.; Hofmann, O.; Walshe, C.A.; Sze, J.Y.Y.; McClean, G.D.; Mosley, A.; Rattle, S.J.; Bradley, D.D.C. Highly sensitive fluorescence detection system for microfluidic lab-on-a-chip. *Lab Chip* **2011**, *11*, 1664–1670.
47. Kamei, T.; Paegel, B.M.; Scherer, J.R.; Skelley, A.M.; Street, R.A.; Mathies, R.A. Integrated hydrogenated amorphous Si photodiode detector for microfluidic bioanalytical devices. *Anal. Chem.* **2003**, *75*, 5300–5305.
48. Kamei, T.; Wada, T. Contact-lens type of micromachined hydrogenated amorphous Si fluorescence detector coupled with microfluidic electrophoresis devices. *Appl. Phys. Lett.* **2006**, *89*, 114101.
49. Lin, C.L.; Lin, H.W.; Wu, C.C. Examining microcavity organic light-emitting devices having two metal mirrors. *Appl. Phys. Lett.* **2005**, *87*, 021101.
50. Peng, H.J.; Sun, J.X.; Zhu, X.L.; Yu, X.M.; Wong, M.; Kwok, H.S. High-efficiency microcavity top-emitting organic light-emitting diodes using silver anode. *Appl. Phys. Lett.* **2006**, *88*, 073517.
51. Dodabalapur, A.; Rothberg, L.J.; Jordan, R.H.; Miller, T.M.; Slusher, R.E.; Phillips, J.M. Physics and applications of organic microcavity light emitting diodes. *J. Appl. Phys.* **1996**, *80*, 6954–6964.
52. Tessler, N.; Harrison, N.T.; Friend, R.H. High peak brightness polymer light-emitting diodes. *Adv. Mater.* **1998**, *10*, 64–68.
53. Shinar, J.; Shinar, R. Organic light-emitting devices (OLEDS) and oled-based chemical and biological sensors: An overview. *J. Phys. D* **2008**, *41*, 133001.
54. Liu, R.; Cai, Y.; Park, J.M.; Ho, K.M.; Shinar, J.; Shinar, R. Organic light-emitting diode sensing platform: Challenges and solutions. *Adv. Funct. Mat.* **2011**, *21*, 4744–4753.
55. Choudhury, B.; Shinar, R.; Shinar, J. Glucose biosensors based on organic light-emitting devices structurally integrated with a luminescent sensing element. *J. Appl. Phys.* **2004**, *96*, 2949–2954.
56. Cai, Y.; Shinar, R.; Zhou, Z.; Shinar, J. Multianalyte sensor array based on an organic light emitting diode platform. *Sensor. Actuat. B* **2008**, *134*, 727–735.
57. Cai, Y.; Smith, A.; Shinar, J.; Shinar, R. Data analysis and aging in phosphorescent oxygen-based sensors. *Sensor. Actuat. B* **2010**, *146*, 14–22.
58. Vohra, V.; Giovanella, U.; Tubino, R.; Murata, H.; Botta, C. Electroluminescence from conjugated polymer electrospun nanofibers in solution processable organic light-emitting diodes. *ACS Nano* **2011**, *5*, 5572–5578.
59. Pagliara, S.; Camposeo, A.; Polini, A.; Cingolani, R.; Pisignano, D. Electrospun light-emitting nanofibers as excitation source in microfluidic devices. *Lab Chip* **2009**, *9*, 2851–2856.
60. Aziz, H.; Liew, Y.F.; Grandin, H.M.; Popovic, Z.D. Reduced reflectance cathode for organic light-emitting devices using metalorganic mixtures. *Appl. Phys. Lett.* **2003**, *83*, 186–188.
61. Wong, F.; Fung, M.; Jiang, X.; Lee, C.; Lee, S. Non-reflective black cathode in organic light-emitting diode. *Thin Solid Films* **2004**, *446*, 143–146.

62. Vannahme, C.; Klinkhammer, S.; Lemmer, U.; Mappes, T. Plastic lab-on-a-chip for fluorescence excitation with integrated organic semiconductor lasers. *Opt. Express* **2011**, *19*, 8179–8186.
63. Camou, S.; Kitamura, M.; Gouy, J.-P.; Fujita, H.; Arakawa, Y.; Fujii, T. Organic Light-Emitting Device as a Fluorescence Spectroscopy Light Source: One Step toward the Lab-on-a-Chip Device. In *Applications of Photonic Technology 5*, Proceedings of SPIE 4833, Quebec City, Quebec, Canada, 2 June 2002; Lessard, R., Lampropoulos, G., Schinn, G., Eds.; SPIE International Society for Optical Engineering: Bellingham, WA, USA, 2003; pp. 1–8.
64. Camou, S.; Kitamura, M.; Arakawa, Y.; Fujii, T. Integration of Oled Light Source And Optical Fibers on a PDMS Based Microfluidic Device for on-Chip Fluorescence Detection. In *7th International Conference on Miniaturized Chemical and Biochemical Analysis Systems*, Proceedings of Micro Total Analysis Systems 2003, Squaw Valley, CA, USA, 5–9 October 2003; Northrup, M., Jensen, K., Harrison, D., Eds.; Transducers Research Foundation: Cleveland Heights, OH, USA, 2003; pp. 383–386.
65. Vengasandra, S.; Cai, Y.K.; Grewell, D.; Shinar, J.; Shinar, R. Polypropylene cd-organic light-emitting diode biosensing platform. *Lab Chip* **2010**, *10*, 1051–1056.
66. Edel, J.B.; Beard, N.P.; Hofmann, O.; Bradley, D.D.C. Thin-film polymer light emitting diodes as integrated excitation sources for microscale capillary electrophoresis. *Lab Chip* **2004**, *4*, 136–140.
67. Hofmann, O.; Wang, X.H.; deMello, J.C.; Bradley, D.D.C.; deMello, A.J. Towards microalbuminuria determination on a disposable diagnostic microchip with integrated fluorescence detection based on thin-film organic light emitting diodes. *Lab Chip* **2005**, *5*, 863–868.
68. Ren, K.N.; Liang, Q.L.; Yao, B.; Luo, G.O.; Wang, L.D.; Gao, Y.; Wang, Y.M.; Qiu, Y. Whole column fluorescence imaging on a microchip by using a programmed organic light emitting diode array as a spatial-scanning light source and a single photomultiplier tube as detector. *Lab Chip* **2007**, *7*, 1574–1580.
69. Yao, B.; Luo, G.; Wang, L.; Gao, Y.; Lei, G.; Ren, K.; Chen, L.; Wang, Y.; Hu, Y.; Qiu, Y. A microfluidic device using a green organic light emitting diode as an integrated excitation source. *Lab Chip* **2005**, *5*, 1041–1047.
70. Yao, B.; Yang, H.; Liang, Q.; Luo, G.; Wang, L.; Ren, K.; Gao, Y.; Wang, Y.; Qiu, Y. High-speed, whole-column fluorescence imaging detection for isoelectric focusing on a microchip using an organic light emitting diode as light source. *Anal. Chem.* **2006**, *78*, 5845–5850.
71. Kim, Y.H.; Shin, K.S.; Kang, J.Y.; Yang, E.G.; Paek, K.K.; Seo, D.S.; Ju, B.K. Poly(dimethylsiloxane)-based packaging technique for microchip fluorescence detection system applications. *J. Microelectromech. Syst.* **2006**, *15*, 1152–1158.
72. Shin, K.S.; Kim, Y.H.; Paek, K.K.; Park, J.H.; Yang, E.G.; Kim, T.S.; Kang, J.Y.; Ju, B.K. Characterization of an integrated, fluorescence-detection hybrid device with photodiode and organic light-emitting diode. *IEEE Electron Device Lett.* **2006**, *27*, 746–748.
73. Devabhaktuni, S.; Prasad, S. Nanotextured organic light emitting diode based chemical sensor. *J. Nanosci. Nanotechnol.* **2009**, *9*, 6299–6306.
74. Scholer, L.; Seibel, K.; Panczyk, K.; Bohm, M. An integrated pled—A light source for application specific lab-on-microchips (ALM). *Microelectron. Eng.* **2009**, *86*, 1502–1504.

75. Nakajima, H.; Okuma, Y.; Morioka, K.; Miyake, M.; Hemmi, A.; Tobita, T.; Yahiro, M.; Yokoyama, D.; Adachi, C.; Soh, N., *et al.* An integrated enzyme-linked immunosorbent assay system with an organic light-emitting diode and a charge-coupled device for fluorescence detection. *J. Sep. Sci.* **2011**, *34*, 2906–2912.
76. Marcello, A.; Sblattero, D.; Cioarec, C.; Maiuri, P.; Melpignano, P. A deep-blue oled-based biochip for protein microarray fluorescence detection. *Biosens. Bioelectron.* **2013**, *46*, 44–47.
77. Wu, X.Z.; Sze, N.S.K.; Pawliszyn, J. Miniaturization of capillary isoelectric focusing. *Electrophoresis* **2001**, *22*, 3968–3971.
78. Cui, H.; Horiuchi, K.; Dutta, P.; Cornelius, F. Isoelectric focusing in a poly (dimethylsiloxane) microfluidic chip. *Anal. Chem.* **2005**, *77*, 1303–1309.
79. Helander, M.; Wang, Z.; Qiu, J.; Greiner, M.; Puzzo, D.; Liu, Z.; Lu, Z. Chlorinated indium tin oxide electrodes with high work function for organic device compatibility. *Science* **2011**, *332*, 944–947.
80. Hofmann, O.; Miller, P.; Sullivan, P.; Jones, T.S.; demello, J.C.; Bradley, D.D.C.; demello, A.J. Thin-film organic photodiodes as integrated detectors for microscale chemiluminescence assays. *Sensor. Actuat. B* **2005**, *106*, 878–884.
81. Wang, X.; Amatatongchai, M.; Nacapricha, D.; Hofmann, O.; de Mello, J.C.; Bradley, D.D.C.; de Mello, A.J. Thin-film organic photodiodes for integrated on-chip chemiluminescence detection–application to antioxidant capacity screening. *Sensor. Actuat. B* **2009**, *140*, 643–648.
82. Wang, X.; Hofmann, O.; Das, R.; Barrett, E.M.; Bradley, D.D.C. Integrated thin-film polymer/fullerene photodetectors for on-chip microfluidic chemiluminescence detection. *Lab Chip* **2006**, *7*, 58–63.
83. Banerjee, A.; Pais, A.; Papautsky, I.; Klotzkin, D. A polarization isolation method for high-sensitivity, low-cost on-chip fluorescence detection for microfluidic lab-on-a-chip. *IEEE Sens. J.* **2008**, *8*, 621–627.
84. Wojciechowski, J.R.; Shriver-Lake, L.C.; Yamaguchi, M.Y.; Füreder, E.; Pieler, R.; Schamesberger, M.; Winder, C.; Prall, H.J.; Sonnleitner, M.; Ligler, F.S. Organic photodiodes for biosensor miniaturization. *Anal. Chem.* **2009**, *81*, 3455–3461.
85. Charwat, V.; Muellner, P.; Hainberger, R.; Purtscher, M.; Ertl, P.; Tedde, S.; Hayden, O. Monitoring Light Scattering Characteristics of Adherent Cell Cultures Using a Lab-on-a-Chip. In *Information Photonics (IP)*, Proceedings of the 2011 ICO International Conference, Ottawa, Canada, 18–20 May 2011; IEEE: Piscataway, NJ, USA, 2011; pp. 1–2.
86. Charwat, V.; Purtscher, M.; Tedde, S.F.; Hayden, O.; Ertl, P. Standardization of microfluidic cell cultures using integrated organic photodiodes and electrode arrays. *Lab Chip* **2013**, *13*, 785–797.
87. Abel, T.; Sagmeister, M.; Lamprecht, B.; Kraker, E.; Kostler, S.; Ungerbock, B.; Mayr, T. Filter-free integrated sensor array based on luminescence and absorbance measurements using ring-shaped organic photodiodes. *Anal. Bioanal. Chem.* **2012**, *404*, 2841–2849.
88. Lamprecht, B.; Sagmeister, M.; Kraker, E.; Hartmann, P.; Jakopic, G.; Köstler, S.; Ditlbacher, H.; Galler, N.; Krenn, J.; Ungerböck, B. Integrated Waveguide Sensor Platform Utilizing Organic Photodiodes. In *Plasmonics in Biology and Medicine IX*, Proceedings of SPIE 8234, San Francisco, CA, USA, 21 January 2012; Vo-Dinh, T., Lakowicz, J. Eds.; SPIE International Society for Optical Engineering: Bellingham, WA, USA, 2012; p. 82341.

89. Lamprecht, B.; Tschepp, A.; Cajlakovic, M.; Sagmeister, M.; Ribitsch, V.; Kostler, S. A luminescence lifetime-based capillary oxygen sensor utilizing monolithically integrated organic photodiodes. *Analyst* **2013**, *138*, 5875–5878.
90. Sagmeister, M.; Lamprecht, B.; Kraker, E.; Haase, A.; Jakopic, G.; Kostler, S.; Ditlbacher, H.; Galler, N.; Abel, T.; Mayr, T. Integrated Organic Optical Sensor Arrays Based on Ring-Shaped Organic Photodiodes. In *Organic Semiconductors in Sensors and Bioelectronics IV*, Proceedings of SPIE 8118, San Diego, CA, USA, 21 August 2011; Shinar, R., Kymissis, I., Eds.; SPIE International Society for Optical Engineering: Bellingham, WA, USA, 2011; p. 811805.
91. Sagmeister, M.; Tschepp, A.; Kraker, E.; Abel, T.; Lamprecht, B.; Mayr, T.; Kostler, S. Enabling luminescence decay time-based sensing using integrated organic photodiodes. *Anal. Bioanal Chem.* **2013**, *405*, 5975–5982.
92. Ishimatsu, R.; Naruse, A.; Liu, R.; Nakano, K.; Yahiro, M.; Adachi, C.; Imato, T. An organic thin film photodiode as a portable photodetector for the detection of alkylphenol polyethoxylates by a flow fluorescence-immunoassay on magnetic microbeads in a microchannel. *Talanta* **2013**, *117*, 139–145.
93. Miyake, M.; Nakajima, H.; Hemmi, A.; Yahiro, M.; Adachi, C.; Soh, N.; Ishimatsu, R.; Nakano, K.; Uchiyama, K.; Imato, T. Performance of an organic photodiode as an optical defector and its application to fluorometric flow-immunoassay for iga. *Talanta* **2012**, *96*, 132–139.
94. Pires, N.M.; Dong, T. Polycarbazole-Based Organic Photodiodes for highly Sensitive Chemiluminescent Immunoassays. In *35th Annual International Conference of the IEEE EMBS*, Proceedings of EMBC 2013, Osaka, Japan, 3–7 July 2013; IEEE: Piscataway, NJ, USA, 2013; pp. 1700–1703.
95. Pires, N.M.; Dong, T. Detection of Stress Hormones by a Microfluidic-Integrated Polycarbazole/Fullerene Photodetector. In *35th Annual International Conference of the IEEE EMBS*, Proceedings of EMBC 2013, Osaka, Japan, 3–7 July 2013; IEEE: Piscataway, NJ, USA, 2013; pp. 4470–4473.
96. Pires, N.M.M.; Dong, T.; Hanke, U.; Hoivik, N. Integrated optical microfluidic biosensor using a polycarbazole photodetector for point-of-care detection of hormonal compounds. *J. Biomed. Opt.* **2013**, *18*, 097001.
97. Pires, N.M.M.; Dong, T. Microfluidic biosensor array with integrated poly (2,7-carbazole)/fullerene-based photodiodes for rapid multiplexed detection of pathogens. *Sensors* **2013**, *13*, 15898–15911.
98. Hofmann, O.; Wang, X.; Cornwell, A.; Beecher, S.; Raja, A.; Bradley, D.D.C. Monolithically integrated dye-doped pdms long-pass filters for disposable on-chip fluorescence detection. *Lab Chip* **2006**, *6*, 981–987.
99. Jorgensen, A.M.; Mogensen, K.B.; Kutter, J.P.; Geschke, O. A biochemical microdevice with an integrated chemiluminescence detector. *Sensor. Actuat. B* **2003**, *90*, 15–21.
100. Blouin, N.; Michaud, A.; Leclerc, M. A low-bandgap poly (2,7-carbazole) derivative for use in high-performance solar cells. *Adv. Mater.* **2007**, *19*, 2295–2300.

101. Park, S.H.; Roy, A.; Beaupré, S.; Cho, S.; Coates, N.; Moon, J.S.; Moses, D.; Leclerc, M.; Lee, K.; Heeger, A.J. Bulk heterojunction solar cells with internal quantum efficiency approaching 100%. *Nat. Photonics* **2009**, *3*, 297–302.
102. Ratcliff, E.L.; Veneman, P.A.; Simmonds, A.; Zacher, B.; Huebner, D.; Saavedra, S.S.; Armstrong, N.R. A planar, chip-based, dual-beam refractometer using an integrated organic light-emitting diode (OLED) light source and organic photovoltaic (OPV) detectors. *Anal. Chem.* **2010**, *82*, 2734–2742.
103. Krishnaswamy, N.; Srinivas, T.; Rao, G.M. Analysis of Integrated Optofluidic Lab-on-a-Chip Fluorescence Biosensor Based on Transmittance of Light Through a Fluidic Gap. In *33rd Annual International Conference of the IEEE EMBS*, Proceedings of EMBC 2011, Boston, MA, USA, 30 August–3 September 2011; IEEE: Piscataway, NJ, USA, 2011; pp. 30–34.
104. Krishnaswamy, N.; Srinivas, T.; Rao, G.M.; Varma, M.M. Analysis of integrated optofluidic lab-on-a-chip sensor based on refractive index and absorbance sensing. *IEEE Sens. J.* **2013**, *13*, 1730–1741.
105. Banerjee, A.; Shuai, Y.; Dixit, R.; Papautsky, I.; Klotzkin, D. Concentration dependence of fluorescence signal in a microfluidic fluorescence detector. *J. Lumines.* **2010**, *130*, 1095–1100.
106. Banerjee, A.; Shuai, Y.; Klotzkin, D.; Papautsky, I. High-Sensitivity Mems Based on-Chip Fluorescence Detection System: Measurement and Analysis of Ultimate Sensitivity Limits. In *2008 17th Biennial University/Government/Industry Micro-Nano Symposium*, Proceedings of the UGIM 2008 Symposium, Louisville, KY, USA, 13–16 July 2008; IEEE: Piscataway, NJ, USA, 2008; pp.177–182.
107. Pais, A.; Banerjee, A.; Klotzkin, D.; Papautsky, I. High-sensitivity, disposable lab-on-a-chip with thin-film organic electronics for fluorescence detection. *Lab Chip* **2008**, *8*, 794–800.
108. Shuai, Y.; Banerjee, A.; Klotzkin, D.; Papautsky, I. On-Chip Fluorescence Detection with Organic Thin Film Devices for Disposable Lab-on-a-Chip Sensors. In *IEEE Sensors 2008*, Proceedings of the Seventh IEEE Sensors Conference 2008, Lecce, Italy, 26–29 October 2008; IEEE: Piscataway, NJ, USA, 2008; pp 122–125.
109. Kraker, E.; Haase, A.; Lamprecht, B.; Jakopic, G.; Konrad, C.; Kostler, S. Integrated organic electronic based optochemical sensors using polarization filters. *Appl. Phys. Lett.* **2008**, *92*, 033302.
110. Mayr, T.; Abel, T.; Kraker, E.; Köstler, S.; Haase, A.; Konrad, C.; Tscherner, M.; Lamprecht, B. An optical sensor array on a flexible substrate with integrated organic opto-electric devices. *Procedia Engineer.* **2010**, *5*, 1005–1008.
111. Liu, R.; Xiao, T.; Cui, W.; Shinar, J.; Shinar, R. Multiple approaches for enhancing all-organic electronics photoluminescent sensors: Simultaneous oxygen and pH monitoring. *Anal. Chim. Acta* **2013**, *778*, 70–78.
112. Nalwa, K.S.; Cai, Y.; Thoeming, A.L.; Shinar, J.; Shinar, R.; Chaudhary, S. Polythiophene-fullerene based photodetectors: Tuning of spectral response and application in photoluminescence based (bio) chemical sensors. *Adv. Mater.* **2010**, *22*, 4157–4161.
113. Lefèvre, F.; Chalifour, A.; Yu, L.; Chodavarapu, V.; Juneau, P.; Izquierdo, R. Algal fluorescence sensor integrated into a microfluidic chip for water pollutant detection. *Lab Chip* **2011**, *12*, 787–793.

114. Ramuz, M.; Leuenberger, D.; Burgi, L. Optical biosensors based on integrated polymer light source and polymer photodiode. *J. Polym. Sci. Pt. B* **2011**, *49*, 80–87.
115. Liang, Y.Y.; Feng, D.Q.; Wu, Y.; Tsai, S.T.; Li, G.; Ray, C.; Yu, L.P. Highly efficient solar cell polymers developed via fine-tuning of structural and electronic properties. *J. Am. Chem. Soc.* **2009**, *131*, 7792–7799.
116. Liang, Y.; Xu, Z.; Xia, J.; Tsai, S.; Wu, Y.; Li, G.; Ray, C.; Yu, L. For the bright future—Bulk heterojunction polymer solar cells with power conversion efficiency of 7.4%. *Adv. Mater.* **2010**, *22*, E135–E138.